

1 RESEARCH ARTICLE

2

3 **Metabolically Distinct Pools of Phosphatidylcholine Are Involved in**  
4 **Trafficking of Fatty Acids out of and into the Chloroplast for**  
5 **Membrane Production**

6

7 **Nischal Karki<sup>a</sup>, Brandon S. Johnson<sup>b</sup>, and Philip D. Bates<sup>a,b,c,2</sup>**

8

9 <sup>a</sup>Department of Chemistry and Biochemistry, University of Southern Mississippi,  
10 Hattiesburg, MS, USA.

11 <sup>b</sup>Institute of Biological Chemistry, Washington State University, Pullman, WA, USA.

12 <sup>c</sup>Corresponding Author: [phil\\_bates@wsu.edu](mailto:phil_bates@wsu.edu)

13

14 **Short title:** Role of LPCAT in leaf acyl trafficking

15

16 **One sentence summary:** Chloroplast lysophosphatidylcholine acyltransferases are  
17 involved in PC acyl editing with newly synthesized fatty acids, and not in  
18 lysophosphatidylcholine transport for galactolipid synthesis.

19

20 **Footnotes:**

21 <sup>1</sup>The author responsible for distribution of materials integral to the findings presented in  
22 this article in accordance with the policy described in the Instructions for Authors  
23 ([www.plantcell.org](http://www.plantcell.org)) is: Philip D. Bates, [phil\\_bates@wsu.edu](mailto:phil_bates@wsu.edu).

24 <sup>2</sup>Current address: Institute of Biological Chemistry, Washington State University,  
25 Pullman, WA, USA

26

27 **ABSTRACT**

28

29 The eukaryotic pathway of galactolipid synthesis involves fatty acid synthesis in  
30 the chloroplast, followed by assembly of phosphatidylcholine (PC) in the endoplasmic  
31 reticulum (ER), and then turnover of PC to provide a substrate for chloroplast  
32 galactolipid synthesis. However, the mechanisms and classes of lipids transported  
33 between the chloroplast and the ER are unclear. PC, PC-derived diacylglycerol,  
34 phosphatidic acid, and lyso-phosphatidylcholine (LPC) have all been implicated in ER-  
35 to-chloroplast lipid transfer. LPC transport requires lysophosphatidylcholine  
36 acyltransferase (LPCAT) activity at the chloroplast to form PC prior to conversion to  
37 galactolipids. However, LPCAT has also been implicated in the opposite chloroplast-to-  
38 ER trafficking of newly synthesized fatty acids through PC acyl editing. To understand  
39 the role of LPC and LPCAT in acyl trafficking we produced and analyzed the  
40 *Arabidopsis thaliana* *act1 lpcat1 lpcat2* triple mutant. *LPCAT1* and *LPCAT2* encode the  
41 major lysophospholipid acyltransferase activity of the chloroplast, and it is  
42 predominantly for incorporation of nascent fatty acids exported from the chloroplast into  
43 PC by acyl editing. *In vivo* acyl flux analysis revealed eukaryotic galactolipid synthesis is  
44 not impaired in *act1 lpcat1 lpcat2* and utilizes a PC pool distinct from that of PC acyl  
45 editing. We present a model for the eukaryotic pathway with metabolically distinct pools

46 of PC, suggesting an underlying spatial organization of PC metabolism as part of the  
47 ER–chloroplast metabolic interactions.

48

## 49 INTRODUCTION

50

51 Membranes that encompass, subdivide, and provide scaffolds for protein  
52 localization are essential to all living cells. In plant leaf tissue, the thylakoid membranes  
53 within the chloroplast are composed predominantly from the galactolipids  
54 monogalactosyldiacylglycerol (MGDG) and digalactosyldiacylglycerol (DGDG) and are  
55 the essential structures that hold the photosynthetic apparatuses. The metabolic  
56 pathways of photosynthetic membrane production have been studied for over 40 years  
57 through biochemical, genetic, and molecular biology approaches and have been  
58 extensively reviewed across the decades (Roughan and Slack, 1982; Browse and  
59 Somerville, 1991; Ohlrogge and Browse, 1995; Moreau et al., 1998; Kelly and Dormann,  
60 2004; Benning, 2008, 2009; Shimojima et al., 2009; Li-Beisson et al., 2013; Boudière et  
61 al., 2014; Hurlock et al., 2014; Block and Jouhet, 2015; Bastien et al., 2016; Botella et  
62 al., 2017; Li-Beisson et al., 2017; LaBrant et al., 2018). This research has led to a  
63 complicated metabolic model that requires the trafficking of lipid substrates from the  
64 chloroplast, to the endoplasmic reticulum (ER), and then back into the chloroplast to  
65 produce galactolipids (Fig. 1). Most of the biosynthetic enzymes and associated genes  
66 of fatty acid synthesis, glycerolipid assembly, and fatty acid desaturation crucial to  
67 produce galactolipids have been identified. However, a major area of uncertainty  
68 surrounds the process of lipid transfer between the chloroplast and the ER, and even  
69 the lipid species that is transferred from the ER back into the plastid is still unclear  
70 (LaBrant et al., 2018).

71 Figure 1 displays the current state of the two-pathway model of leaf MGDG  
72 synthesis (for more detailed comprehensive recent reviews please see (Li-Beisson et  
73 al., 2013; Hurlock et al., 2014; Botella et al., 2017; Li-Beisson et al., 2017; LaBrant et  
74 al., 2018)). Fatty acids are synthesized up to 18-carbon saturated or monounsaturated  
75 fatty acids while esterified to acyl carrier protein (ACP) within the chloroplast stroma. In  
76 some plants these acyl-ACPs can be utilized by the acyl selective glycerol-3-phosphate  
77 acyltransferase (GPAT) and lysophosphatidic acid acyltransferase (LPAT) of the

78 “prokaryotic pathway” (*ACT1/ATS1* and *ATS2*, respectively (Kunst et al., 1988; Nishida  
79 et al., 1993; Yu et al., 2004)) to produce a molecular species of phosphatidic acid (PA)  
80 containing oleate (18:1, number carbons: number double bonds) at the *sn*-1 position,  
81 and palmitate (16:0) at the *sn*-2 position. Dephosphorylation produces the diacylglycerol  
82 (DAG) substrate of MGDG synthase (MGD1) (Jarvis et al., 2000). Subsequent  
83 desaturation of the 18:1/16:0 molecular species to 18:3/16:3 produces the abundant  
84 polyunsaturated molecular species of MGDG characteristic of chloroplast membranes.

85 Plants that produce up to half of the MGDG through the prokaryotic pathway are  
86 known as 16:3 plants in reference to the 16:3 that accumulates at *sn*-2 of MGDG. Only  
87 about 12% of Angiosperms (including *Arabidopsis thaliana*) are 16:3 plants (Mongrand  
88 et al., 1998). In contrast to 16:3 plants, 18:3 plants accumulate 18:3 at the *sn*-2 position  
89 of MGDG through glycerolipid assembly by the ER-localized “eukaryotic pathway”  
90 where *sn*-2 acyltransferases are selective for 18-carbon unsaturated fatty acids. In all  
91 plants, the eukaryotic pathway GPAT and LPAT (*AtGPAT9* and *AtLPAT2*, respectively  
92 (Kim et al., 2005; Shockley et al., 2016; Singer et al., 2016)) utilize cytosolic acyl-CoA to  
93 produce PA, and DAG in a parallel pathway to that in chloroplast (Fig. 1). The *de novo*  
94 synthesized DAG is utilized to produce ER phospholipids such as phosphatidylcholine  
95 (PC) and phosphatidylethanolamine (PE). PC is also the extra-plastidic site for  
96 desaturation of 18:1, to 18:2 and 18:3 through the FAD2 and FAD3 enzymes,  
97 respectively (Arondel et al., 1992; Okuley et al., 1994). Eukaryotic MGDG is synthesized  
98 from a polyunsaturated DAG backbone derived from PC (Slack et al., 1977). However,  
99 the mechanism and location of PC turnover, and the lipid class transferred from the ER  
100 to the chloroplast are still unclear (Fig. 1, blue dashed lines). A key aspect of the  
101 eukaryotic pathway is that extensive trafficking of acyl groups between the chloroplast  
102 and the ER is required.

103 Fatty acid export from the chloroplast begins with hydrolysis of acyl-ACPs by  
104 fatty acid thioesterases (Fig. 1) (Bates et al., 2013). The subsequent free fatty acids  
105 (FFA) are transported across the chloroplast inner envelope membrane (IEM) by FAX1  
106 (Li et al., 2015), and likely other members of the FAX family. The mechanism of FFA  
107 transfer across the chloroplast outer envelope membrane (OEM) is not clear but may  
108 involve vectoral diffusion driven by activation of FFA to acyl-CoA by long chain acyl-

109 coenzyme A synthetases (LACS) on the cytoplasmic side of the OEM and/or the ER  
110 (Schnurr et al., 2002; Koo et al., 2004; Zhao et al., 2010; Jessen et al., 2015), which  
111 prevents FFA diffusion back into the plastid. Original models of the eukaryotic pathway  
112 assumed acyl-CoA-containing newly synthesized fatty acids were utilized by the ER-  
113 localized GPAT and LPAT to produce initial molecular species of glycerolipids  
114 containing 16:0 or 18:1 at *sn*-1, and 18:1 at *sn*-2 prior to further desaturation on PC (e.g.  
115 (Ohlrogge and Browse, 1995)). However, metabolic tracing experiments in various plant  
116 tissues have demonstrated that the majority of newly synthesized fatty acids exported  
117 from the plastid are initially rapidly incorporated into PC by a process known as acyl  
118 editing, which is essentially an acyl-CoA:PC fatty acid exchange cycle (Williams et al.,  
119 2000; Bates et al., 2007; Bates et al., 2009; Bates et al., 2012; Tjellström et al., 2012;  
120 Yang et al., 2017). This exchange between PC and the acyl-CoA pool produces a  
121 mixture of nascent fatty acids exported from the plastid with previously synthesized fatty  
122 acids derived from PC, some of which may have been desaturated to 18:2, or 18:3. This  
123 mixed acyl-CoA pool is thus the substrate for the eukaryotic GPAT and LPAT reactions  
124 for *de novo* glycerolipid assembly. In particular, short time point ( $\leq 1$  min) [ $^{14}\text{C}$ ]acetate  
125 labeling of fatty acid synthesis in pea (*Pisum sativum*) leaves and *Arabidopsis* cells was  
126 crucial to demonstrating that nascent fatty acids are predominantly incorporated into the  
127 *sn*-2 position of PC by a lysophosphatidylcholine acyltransferase (LPCAT)-type reaction  
128 faster than incorporation into *de novo* DAG of the eukaryotic pathway (Bates et al.,  
129 2007; Tjellström et al., 2012). These results suggest that the lysophosphatidylcholine  
130 (LPC) pool and LPCAT enzymes involved in acyl editing may be part of the acyl  
131 trafficking of nascent fatty acids from the chloroplast to the ER (Fig. 1).

132 The lipids DAG, PA, PC, and LPC have all been suggested as the species  
133 transported from the ER to the chloroplast in the eukaryotic pathway (Fig. 1). DAG was  
134 first suggested to be transferred from the ER to the plastid after metabolic labeling  
135 experiments indicated that both the glycerol and fatty acids of PC were incorporated into  
136 MGDG together (Slack et al., 1977), and analysis of *Arabidopsis* PA hydrolase mutants  
137 (*pah1* and *pah2*) under phosphate starvation supported this conclusion (Nakamura et  
138 al., 2009). However, combining the *pah1* and *pah2* mutants with the *act1* mutation  
139 which eliminates the prokaryotic pathway did not appear to affect eukaryotic galactolipid

140 synthesis under phosphate replete conditions (Fan et al., 2014). Recent work  
141 characterizing the *Arabidopsis tgd1-5* mutants has indicated a transporter system  
142 involved in transferring the lipid substrate for MGDG synthesis from the chloroplast  
143 OEM to the IEM where MGDG synthesis occurs (Xu et al., 2003; Xu et al., 2005; Awai  
144 et al., 2006; Lu et al., 2007; Wang et al., 2012b; Wang et al., 2013; Fan et al., 2015).  
145 The mutants have impaired eukaryotic MGDG production and accumulate unusual  
146 trigalactosyldiacylglycerols (TGDG) as a phenotype. The TGD2 and TGD4 components  
147 of this transporter system bind to PA, and isolated chloroplasts from the *tdg1* mutant  
148 effectively convert exogenous DAG into MGDG but exogenous PA conversion to MGDG  
149 is partially reduced. Therefore, PA has been proposed as the molecule transported from  
150 the ER to the plastid (Xu et al., 2005; Lu and Benning, 2009; Wang et al., 2012b; Wang  
151 et al., 2013). However, it is also been suggested that the role of PA is to destabilize  
152 membranes to reduce the energy barrier to transport of a different lipid species (LaBrant  
153 et al., 2018). A recent mathematical modeling approach suggested DAG was a better  
154 substrate to transport than PA, but limited PA transport was also required to activate  
155 MGDG synthesis (Maréchal and Bastien, 2014). Both DAG and PA can be produced by  
156 lipases in the ER, and thus could be transferred from the ER to the chloroplast and then  
157 into the IEM for MGDG synthesis. A different approach would be to first move PC from  
158 the ER to the chloroplast, and then derive PA or DAG from PC for transport to the IEM  
159 by the mechanisms discussed above.

160 PC is highly abundant in the outer leaflet of the OEM but is not present in other  
161 chloroplast membranes (Dorne et al., 1985), while the ER lipid PE is absent from  
162 chloroplasts. PC can be selectively transferred over PE from liposomes to isolated  
163 chloroplasts, a process which is dependent on the proteins within the chloroplast OEM  
164 (Yin et al., 2015), suggesting PC could be directly transferred from the ER, possibly  
165 through ER-chloroplast membrane contact sites (Andersson and Dörmann, 2008;  
166 Mueller-Schuessele and Michaud, 2018). Recent characterization of the flippase ALA10  
167 (Botella et al., 2016) suggests it could be involved in enriching PC in ER membrane  
168 contact sites prior to transfer to the plastid (Botella et al., 2017). Rather than trafficking  
169 of a whole membrane lipid, LPC is a more water-soluble derivative of PC that could  
170 more easily traverse an aqueous space between the two compartments. The abundant

171 LPCAT activities associated with the exterior of the chloroplast would then regenerate  
172 PC at the OEM (Bessoule et al., 1995; Tjellström et al., 2012). The transfer of LPC from  
173 the ER to plastid was supported by long time point (2–100 h) pulse-chase metabolic  
174 labeling studies in leek seedlings, which demonstrated a loss of fatty acids from *sn*-  
175 1/*sn*-2 PC and the subsequent accumulation in mostly *sn*-1 MGDG (Mongrand et al.,  
176 1997; Mongrand et al., 2000). The authors concluded that it was labeled *sn*-1-acyl-LPC  
177 that was transferred to the chloroplast and then reacylated with unlabeled fatty acids by  
178 LPCAT at the OEM during the chase in route to MGDG production. These results  
179 suggest that LPC and chloroplast LPCAT activity may be part of the ER-to-chloroplast  
180 lipid transfer reactions of the leaf eukaryotic pathway.

181 The discussion of previous research above indicates that LPC and LPCAT  
182 activity may have roles in both trafficking of fatty acids from the chloroplast to the ER,  
183 and from the ER to the chloroplast. Arabidopsis has four enzymes with demonstrated *in*  
184 *vitro* LPCAT activity: AtLPCAT1 and AtLPCAT2 (Stahl et al., 2008; Wang et al., 2012a;  
185 Lager et al., 2013; Wang et al., 2014), and the lysophosphatidylethanolamine  
186 acyltransferases AtLPEAT1 and AtLPEAT2 (Stalberg et al., 2009; Jasieniecka-  
187 Gazarkiewicz et al., 2016). AtLPCAT1 and AtLPCAT2 have a strong preference for 18-  
188 carbon unsaturated acyl-CoAs over 16:0-CoA, and thus could produce the *sn*-1/2 18-  
189 carbon molecular species of PC (and subsequent MGDG) characteristic of the  
190 eukaryotic pathway (Lager et al., 2013). Short timepoint metabolic tracing of lipid  
191 metabolism in developing seeds of the LPCAT1 LPCAT2 double mutant (*lpcat1 lpcat2*)  
192 indicated the initial incorporation of nascent fatty acids into PC through *sn*-2 acyl editing  
193 was abolished (Bates et al., 2012). Instead the acyl groups are rerouted and initially  
194 esterified to G3P through the GPAT and LPAT reactions of the eukaryotic pathway prior  
195 to *de novo* PC synthesis. This result suggests that the Arabidopsis LPCAT1 and  
196 LPCAT2 enzymes are involved in the flux of acyl groups from the plastid to the ER in  
197 developing seeds, and that LPEAT1 and LPEAT2 cannot compensate for the loss of  
198 LPCATs in the acyl-editing cycle. However, these previous results are not directly  
199 applicable to leaves for two reasons: (1) In developing seeds LPCAT1 and LPCAT2 are  
200 expressed at 2-3 fold higher levels than LPEAT1 and LPEAT2 (Supplemental Fig. 1)  
201 which may explain the lack of compensatory acyl-editing activity by LPEAT1 and

202 LPEAT2 in the *lpcat1 lpcat2* mutant seeds. In leaves LPEAT1 and LPEAT2 are  
203 expressed at similar or even higher levels than LPCAT1 and LPCAT2 (Supplemental  
204 Fig. 1). Therefore, it is possible that LPCAT1/LPCAT2 and LPEAT1/LPEAT2 may both  
205 contribute the acyl-editing LPCAT activity in leaves. (2) Quantitative acyl flux between  
206 the plastid and the ER is distinctly different between developing leaves and developing  
207 oilseed tissues. In leaves of 18:3 plants >60% of all fatty acids exported to the ER are  
208 reincorporated into the plastid for chloroplast membrane production. However, in  
209 oilseeds the major flux of acyl groups is for ER-localized triacylglycerol (TAG) synthesis  
210 such that >95% of acyl groups accumulate in extra-plastidial oil bodies and membranes,  
211 with very little flux back into the plastid (Li-Beisson et al., 2013). Thus, previous acyl flux  
212 studies on developing seeds of *lpcat1 lpcat2* are not appropriate for measuring the role  
213 of LPCATs in the flux of acyl groups from the ER to the plastid for galactolipid  
214 production in leaves.

215 Therefore, to understand the roles of LPC and LPCAT activity in acyl flux to and  
216 from the ER and chloroplast we crossed the Arabidopsis *lpcat1 lpcat2* double mutant  
217 (Bates et al., 2012) with the *act1* mutant (Kunst et al., 1988). *ACT1* (also called *ATS1*  
218 (Nishida et al., 1993)) encodes the chloroplast GPAT. The *act1* mutant eliminates  
219 prokaryotic pathway MGDG synthesis and enhances acyl flux through the eukaryotic  
220 pathway, similar to 18:3 plants. Our analysis of lipid accumulation, chloroplast-  
221 associated LPCAT activity, and *in vivo* acyl fluxes through both short timepoint  
222 metabolic tracing and long timepoint pulse-chase experiments further clarify the role of  
223 LPCATs within leaf PC acyl editing, and distinguish a separate metabolically-active pool  
224 of PC involved in providing the substrate for chloroplast lipid synthesis.

225

## 226 **RESULTS**

227

### 228 **Production and characterization of the *act1 lpcat1 lpcat2* triple mutant**

229

230 In Arabidopsis leaves both the eukaryotic pathway and prokaryotic pathway  
231 contribute approximately equally to MGDG production (Browse et al., 1986). To better  
232 understand the roles of LPCAT1 and LPCAT2 specifically in eukaryotic pathway

galactolipid production we crossed the *lpcat1 lpcat2* double mutant (Bates et al., 2012) with the *act1* mutant, which essentially eliminates prokaryotic pathway galactolipid production (Kunst et al., 1988). The *act1* allele is partially leaky, and residual GPAT activity remaining in the chloroplast is utilized for phosphatidylglycerol (PG) production (Xu et al., 2006). Previous crosses of *act1* with *tgd1-1* (a component of the transporter complex that imports the eukaryotic pathway lipid substrate into the chloroplast) was embryo lethal (Xu et al., 2005). We reasoned if the transport of LPC to chloroplasts and its subsequent conversion to PC by LPCAT at the chloroplast OEM was a key part of the eukaryotic pathway, then the *act1 lpcat1 lpcat2* triple mutant may also demonstrate developmental or vegetative growth defects. Crossed F1 seeds were grown to maturity, and seed was collected and re-sown. The segregating F2 plants were screened for homozygosity of the *lpcat1 lpcat2* double T-DNA mutation by PCR, and for homozygosity of the *act1* mutation by the lack of 16:3 in leaf lipids by gas chromatography (Kunst et al., 1988). During the initial screening no growth phenotypes were observed. Homozygous *act1 lpcat1 lpcat2* triple mutants were subsequently grown side-by-side with parental lines and wild-type Col-0. Across vegetative growth, the size of the triple mutants was within the plant-to-plant variation range of the parental lines (Supplemental Fig. 2). Therefore, the *act1 lpcat1 lpcat2* triple mutation has minimal effects on plant vegetative growth.

To determine if the *act1 lpcat1 lpcat2* triple mutant had defects in leaf lipid production we measured the relative accumulation of leaf membrane lipids at three developmental stages (2, 3, and 4 weeks after germination) in four lines of *Arabidopsis*: wild-type Col-0, *act1*, *lpcat1 lpcat2* double mutant, and the *act1 lpcat1 lpcat2* triple mutant (Fig. 2). In general the relative accumulation of leaf membrane lipids in the *lpcat1 lpcat2* mutant was similar to Col-0; however as previously characterized, the *act1* mutant has a significant change from Col-0 with less MGDG and PG, and a corresponding increase in PC and DGDG (Fig. 2A-C) (Kunst et al., 1988). Therefore, to understand the effect of the *lpcat1 lpcat2* mutation when acyl flux through the eukaryotic pathway is enhanced in the *act1* background, our main comparison is between *act1* and the *act1 lpcat1 lpcat2* triple mutant. At two and three weeks there were no significant changes in membrane lipid abundance between the two lines (Fig. 2A-B). At four weeks

264 (Fig. 2C), only PG demonstrated a significant increase from  $2.2\% \pm 1.0\%$  in the *act1* line  
265 to  $10.1 \pm 3.1\%$  in the *act1 lpcat1 lpcat2* line (P-value = 0.0013).

266 Even though the amount of PC or PE did not significantly change between *act1*  
267 and *act1 lpcat1 lpcat2*, there were significant changes to their fatty acid compositions,  
268 especially at later stages in development (Fig. 3). There was no change in either PC or  
269 PE at 2 weeks after germination (Fig. 3A, 3D). At 3 weeks PC 18:1 content decreased  
270 from  $23.1\% \pm 0.3\%$  in the *act1* line to  $18.5\% \pm 0.05\%$  in the *act1 lpcat1 lpcat2* line (Fig.  
271 3B). At 4 weeks PC 18:1 decreased from  $29.7\% \pm 1.1\%$  in *act1* to  $20.8\% \pm 0.6\%$  in *act1*  
272 *lpcat1 lpcat2*, which was mostly compensated for by significant increases in 18:2 (from  
273  $37.8\% \pm 0.9\%$  to  $42.4\% \pm 0.4\%$ ) and 18:3 (from  $15.6\% \pm 0.3\%$  to  $17.8\% \pm 0.5\%$ ). The  
274 only significant change in PE between *act1* and *act1 lpcat1 lpcat2* was at 4 weeks (Fig.  
275 3F), where 16:0 decreased (from  $27.0\% \pm 0.3\%$  to  $25.1\% \pm 0.3\%$ ), 18:2 decreased  
276 (from  $43.1\% \pm 0.7\%$  to  $40.7\% \pm 0.5\%$ ), and 18:3 increased (from  $13.6\% \pm 0.4\%$  to  
277  $16.6\% \pm 0.7\%$ ). Supplemental Figures 3, 4 and 5 report the fatty acid composition for all  
278 other lipids measured in Fig. 2 at 2, 3, and 4 weeks respectively. The major galactolipid  
279 products of the eukaryotic pathway (MGDG and DGDG) did not have any significant  
280 changes in fatty acid composition between *act1* and *act1 lpcat1 lpcat2*. The change in  
281 abundance of PG measured at 4 weeks (Fig. 2C), only had a limited effect on its fatty  
282 acid composition with a significant increase in 18:3 in the *act1 lpcat1 lpcat2* line (from  
283  $30.7\% \pm 0.3\%$  to  $32.3\% \pm 0.1\%$ ).

284 Together, the limited effect of the *act1 lpcat1 lpcat2* triple mutation compared to  
285 the *act1* mutation alone on plant growth and lipid accumulation across leaf development  
286 suggests that LPCAT1 and LPCAT2 are not essential for eukaryotic pathway lipid  
287 metabolism when the prokaryotic pathway is limiting. However, other lysophospholipid  
288 acyltransferases (such as LPEAT1 and LPEAT2) have demonstrated LPCAT activity *in*  
289 *vitro* (Stalberg et al., 2009; Jasieniecka-Gazarkiewicz et al., 2016), and are expressed  
290 at similar levels to *LPCAT1* *LPCAT2* in leaves (Supplemental Fig. 1). Thus, it is possible  
291 that other lysophospholipid acyltransferases may compensate for the loss of LPCAT  
292 activity in the *act1 lpcat1 lpcat2* background. *In vitro* LPCAT activity has also been  
293 associated with multiple subcellular membrane fractions (Bessoule et al., 1995;  
294 Tjellström et al., 2012; Wang et al., 2014). To measure if the chloroplast-associated

295 LPCAT activity that has been hypothesized to be involved in the eukaryotic pathway of  
296 galactolipid synthesis (Mongrand et al., 1997; Moreau et al., 1998; Mongrand et al.,  
297 2000) is actually reduced in the *lpcat1 lpcat2* mutants, we performed LPCAT assays on  
298 chloroplasts isolated from each plant line (Fig. 4). The controls Col-0 and *act1* did not  
299 exhibit a significant difference in the LPCAT activity that produced [<sup>14</sup>C]PC from the  
300 addition of LPC and [<sup>14</sup>C]oleoyl-CoA to the isolated chloroplasts. However, [<sup>14</sup>C]PC  
301 production was reduced ~85% in *act1 lpcat1 lpcat2* from wild-type levels (Fig. 4).

302 There was also no significant difference in [<sup>14</sup>C]PC synthesis between *lpcat1*  
303 *lpcat2* and *act1 lpcat1 lpcat2* lines. It is not clear if the residual [<sup>14</sup>C]PC synthesis within  
304 the *lpcat1 lpcat2* backgrounds is chloroplast-localized LPCAT activity, or if it is due to  
305 the activity of other lysophospholipid acyltransferases from partial contamination of the  
306 isolated chloroplasts with other cellular membrane fractions (Larsson et al., 2007;  
307 Stalberg et al., 2009; Bulat and Garrett, 2011; Jasieniecka-Gazarkiewicz et al., 2016).  
308 Nevertheless, the major chloroplast-associated LPCAT activity in the *act1 lpcat1 lpcat2*  
309 triple mutant was mostly eliminated (Fig. 4), and it had little to no effect on growth or leaf  
310 galactolipid accumulation (Fig. 2, Supplemental Fig. 2), suggesting LPCAT activity is not  
311 an essential part of eukaryotic pathway galactolipid synthesis. However, the mass  
312 accumulation of MGDG and DGDG does not indicate the metabolic pathway of  
313 synthesis. To better understand how the loss of the major chloroplast LPCAT activity  
314 affects acyl flux out of the chloroplast and through the eukaryotic pathway into  
315 galactolipids of the *act1 lpcat1 lpcat2* triple mutant, we moved on to an *in vivo* metabolic  
316 labeling approach during the stage of rapid leaf growth (3-week-old plants).

317

318 **Rapid *in vivo* metabolic labeling to characterize the effect of *lpcat1 lpcat2* on the  
319 entry of nascent fatty acids into the eukaryotic pathway through acyl editing**

320

321 Newly synthesized fatty acids produced in the stroma of the plastid are exported  
322 as free fatty acids and esterified to co-enzyme A in the ER for use by the various  
323 acyltransferases of the eukaryotic pathway (Li-Beisson et al., 2013). Rapid metabolic  
324 labeling experiments in leaves, seeds, and plant suspension cells have demonstrated  
325 that nascent fatty acids exported from the plastid are predominantly directly

326 incorporated into PC through an LPCAT-type reaction within the acyl-editing cycle,  
327 rather than first esterified to glycerol-3-phosphate through *de novo* glycerolipid  
328 biosynthesis (Bates et al., 2007; Bates et al., 2009; Bates et al., 2012; Tjellström et al.,  
329 2012; Yang et al., 2017). This rapid incorporation into PC may take place on the  
330 chloroplast surface where significant LPCAT activity resides and ER-plastid connection  
331 sites are present (Andersson et al., 2007; Tjellström et al., 2012; Botella et al., 2017).  
332 We demonstrated that the *lpcat1 lpcat2* knockout eliminates most of the chloroplast-  
333 associated LPCAT activity (Fig. 4). To determine if the knockout of *lpcat1 lpcat2* also  
334 affects the initial incorporation of nascent fatty acids into the eukaryotic pathway through  
335 PC acyl editing, we followed the continual incorporation of [<sup>14</sup>C]acetate into fatty acid  
336 synthesis and lipid assembly (Allen et al., 2015) in developing leaves of *act1* and *act1*  
337 *lpcat1 lpcat2* over a short time course from 5 to 60 min (Fig. 5). [<sup>14</sup>C]acetate  
338 incorporation into total lipids was linear and had the same rate of accumulation in each  
339 line (Fig. 5A). However, on average *act1* had more total DPM/μg chlorophyll than *act1*  
340 *lpcat1 lpcat2*. Higher accumulation of label but with the same rate may be due to a  
341 difference in [<sup>14</sup>C]acetate concentration in the incubation medium for each line, or  
342 possibly a small difference in total chlorophyll content utilized for normalization.  
343 Accumulation of <sup>14</sup>C labeled fatty acids into different glycerolipids was also linear,  
344 indicating continuous biosynthesis of each lipid over the time course in each line (Fig.  
345 5B-C). Together these results indicate similar rates of total fatty acid biosynthesis in  
346 each line, and no indication of lipid degradation during the time course.

347 The relative accumulation of labeled lipids in *act1* and *act1 lpcat1 lpcat2* from  
348 Figure 5 is shown in Figure 6. At 60 min the relative labeling between lipids was similar  
349 in both lines; however, the initial incorporation of nascent fatty acids into PC of the *act1*  
350 *lpcat1 lpcat2* line was delayed compared to *act1* (Fig. 6A). The decrease in PC was  
351 mostly compensated for by significant increases in DAG and PE (Fig. 6B-C). There was  
352 no significant difference measured between the lines for labeling of PA, PG, and PI/PS  
353 (Fig. 6B-C), and notably MGDG (Fig. 6D).

354 To gain a better understanding of the mechanisms of newly synthesized fatty  
355 acid incorporation into the eukaryotic pathway, we characterized the positional  
356 distribution of the <sup>14</sup>C-labeled fatty acids in PC and DAG across the labeling time course

357 for both *act1* and *act1 lpcat1 lpcat2* (Fig. 7). In *act1* DAG contained similar amounts of  
358 nascent fatty acids at both stereochemical positions with a slight preference for *sn*-1  
359 (55-60%) over *sn*-2 (40-45%) across the time course (Fig. 7A). In the PC of *act1* most of  
360 the nascent fatty acids accumulated at the *sn*-2 position (~75%) at all time points (Fig.  
361 7C). In *act1 lpcat1 lpcat2*, DAG stereochemical labeling was similar to that of DAG in  
362 *act1* with a slight preference for the *sn*-1 position (Fig. 7B). However, PC of *act1 lpcat1*  
363 *lpcat2* was distinctly different than *act1* PC, with the stereochemical labeling  
364 demonstrating a preference for *sn*-1 labeling (~60%) across the time course, similar to  
365 DAG from both lines. The rapid incorporation of nascent fatty acids predominantly in *sn*-  
366 2 of PC of *act1* (Fig. 5B, Fig. 7C) is characteristic of newly synthesized fatty acids first  
367 entering eukaryotic glycerolipids through PC acyl editing. However, in *act1 lpcat1 lpcat2*  
368 the initial delay of PC labeling and increase of DAG labeling (Fig. 5C, 6A-B), combined  
369 with the similar stereochemical labeling of PC and DAG across the time course (Fig. 7B,  
370 7D) is consistent with an elimination of nascent fatty acid entry into eukaryotic  
371 glycerolipids through PC acyl editing and a reorientation of acyl flux to first move  
372 through DAG then into PC. These results indicate that LPCAT1 and LPCAT2 are  
373 involved in the direct incorporation of nascent fatty acids into PC through acyl editing as  
374 the fatty acids exit the chloroplast, and that other lysophospholipid acyltransferases do  
375 not compensate for the loss of LPCAT1 and LPCAT2 activity in the leaf acyl editing  
376 cycle.

377

378 **Pulse-chase metabolic labeling to characterize the effect of *lpcat1 lpcat2* on the**  
379 **PC–MGDG precursor–product relationship of the eukaryotic pathway**

380

381 To measure acyl flux through the longer-term precursor–product relationships  
382 within leaf lipid metabolism, we performed a pulse-chase metabolic tracing experiment.  
383 Three-week-old rosettes from both the *act1* and *act1 lpcat1 lpcat2* lines were pulsed  
384 with [<sup>14</sup>C]acetate for 15 min, the radioisotope was washed off, and then the samples  
385 were chased without radiolabel for an additional 51 h to measure the redistribution of  
386 fatty acids as eukaryotic pathway intermediates turn over with time (Fig. 8). Similar to  
387 the short-timepoint continuous [<sup>14</sup>C]acetate labeling experiment (Fig. 5, 6), at the end of

388 the pulse most of the newly synthesized radioactive fatty acids were in PC in both the  
389 *act1* (Fig. 8A) and *act1 lpcat1 lpcat2* (Fig. 8B) lines. During the chase the radioactivity in  
390 PC rapidly declined, and the fatty acids were redistributed predominantly into MGDG,  
391 followed by PE, and then TAG. All other measured lipids (PG, PA, DAG, PI/PS, DGDG)  
392 contained only minor amounts of radioactivity over the chase period (Fig. 8A-B). When  
393 the relative labeling of individual lipids was compared between the plant lines, there was  
394 no statistical difference in the labeling pattern for the major labeled lipids PC, MGDG,  
395 and PE. PC levels differed only at the 51 h time point where there was more labeled PC  
396 in *act1 lpcat1 lpcat2* than in *act1* (Fig. 8C-E). In addition, there was no difference  
397 between the lines over the time course for labeling of DAG (Fig. 8C) and PA (Fig. 8E),  
398 which are intermediates of glycerolipid synthesis. This result suggests that the  
399 quantitative turnover of PC to provide the substrate for MGDG synthesis within the  
400 eukaryotic pathway is not affected by the *lpcat1 lpcat2* mutations.

401 Interestingly, TAG labeling was significantly different between the two plant lines  
402 (Fig. 8F). TAG accumulation is very minor in leaf tissue under normal circumstances  
403 (typically < 1% of total lipid mass), but a dynamic small pool of TAG that is constantly  
404 synthesized and degraded can be measured through radiolabeling (Fan et al., 2014;  
405 Tjellström et al., 2015). Both lines demonstrated the same trend, with the continual  
406 increase of labeled fatty acid in TAG until the 22 h timepoint, and then a decrease  
407 through the remaining time course. However, starting at the 4 h timepoint the *act1* line  
408 had a significantly higher proportion of labeled fatty acids in TAG than the *act1 lpcat1*  
409 *lpcat2* line did (Fig. 8F).

410 To gain a better understanding of the role of the LPCAT1 LPCAT2 enzymes in  
411 leaf eukaryotic pathway metabolism, we analyzed the changes in both the labeled fatty  
412 acid composition (Fig. 9), and their stereochemical location (Fig. 10) within DAG, PC,  
413 and MGDG across the [<sup>14</sup>C]acetate pulse-chase time course (Fig. 8). DAG, PC, and  
414 MGDG each had a unique profile of <sup>14</sup>C-fatty acid accumulation. However, when the  
415 composition of labeled fatty acids within each lipid was compared between the *act1* and  
416 *act1 lpcat1 lpcat2* lines there was no significant differences between the lines (Fig. 9).  
417 There was limited change in the composition of DAG over the 51 h chase period (Fig.  
418 9A-B), consistent with its role as an intermediate of lipid metabolism that is not a

419 substrate of fatty acid desaturases. However, PC and MGDG had larger changes in  
420 composition as both lipid classes are substrates for desaturases, and the acyl groups  
421 that are initially incorporated into PC eventually accumulate in MGDG (Fig. 8). In PC the  
422 major change in composition was a decrease in monoenoic fatty acids, with a  
423 concomitant increase in both dienoic and trienoic fatty acids as a proportion of the  
424 labeled fatty acids remaining in PC (Fig. 9C-D). The major change in MGDG was a  
425 large increase in trienoic fatty acids (Fig. 9F). Considering the precursor–product  
426 relationship of acyl transfer between PC and MGDG (Fig. 8), these results are  
427 consistent with the loss of nascent  $^{14}\text{C}$ -18:1 initially incorporated into PC (through both  
428 desaturation and acyl transfer) and its subsequent accumulation as  $^{14}\text{C}$ -18:3 in MGDG.  
429 These results are consistent with the current understanding of the eukaryotic pathway  
430 (Fig. 1). Together with Figure 8, this result suggests the *lpcat1 lpcat2* mutations have  
431 little to no effect on the flux of total acyl groups (Fig. 8) or select fatty acids (Fig. 9) from  
432 PC to MGDG within the eukaryotic pathway.

433 Despite the similarities of acyl accumulation and composition over the pulse-  
434 chase between the *act1* and *act1 lpcat1 lpcat2* lines, the stereochemical location of the  
435 labeled acyl groups revealed significant differences between the lines (Fig. 10). During  
436 the pulse-chase experiment labeled DAG can represent *de novo* DAG at early time  
437 points. At later time points labeled DAG can represent *de novo* DAG synthesized with  
438 fatty acids removed from other lipids, and DAG derived from membrane lipid or TAG  
439 turnover. The  $^{14}\text{C}$ -fatty acid stereochemistry in DAG throughout the pulse-chase time  
440 course indicated more labeled fatty acids at the *sn*-1 position than the *sn*-2 position (Fig.  
441 10A), similar to the short timepoint continuous  $[^{14}\text{C}]$ acetate labeling experiment (Fig. 7A-  
442 B). There was no significant difference between *act1* or *act1 lpcat1 lpcat2* at any time  
443 point, indicating the loss of LPCAT1 LPCAT2 does not affect initial or prolonged DAG  
444 metabolism. The *act1* PC stereochemistry was similar to the continuous labeling  
445 experiment (Fig. 7C) throughout the pulse-chase with more  $^{14}\text{C}$ -fatty acids at *sn*-2 than  
446 *sn*-1 (Fig. 10B), consistent with the incorporation of nascent fatty acids into *sn*-2 PC by  
447 LPCAT-mediated acyl editing. The *act1 lpcat1 lpcat2* PC stereochemistry was initially  
448 similar to the short timepoint continuous labeling experiment (Fig. 7D) with more label at  
449 *sn*-1 than *sn*-2, consistent with the loss of rapid incorporation of nascent fatty acids into

450 PC through acyl editing. However, after 4 hours of chase there was a switch in  
451 stereochemistry, with more labeled fatty acids in the *sn*-2 position rather than the *sn*-1  
452 (Fig. 10B), more similar to PC from the *act1* mutant. At all timepoints the labeled fatty  
453 acid stereochemistry in PC was significantly different between the *act1* and *act1 lpcat1*  
454 *lpcat2* lines. For MGDG, the early timepoints indicated similar stereochemical  
455 localization of the  $^{14}\text{C}$ -fatty acids in both lines, at later time points in the chase more *sn*-  
456 1 labeled fatty acids accumulated in both lines (Fig. 10C). It is important to point out that  
457 MGDG accumulated as the major labeled lipid by the end of the chase period (Fig. 8A-  
458 B), and that the stereochemistry of labeled acyl groups was similar to that of DAG  
459 throughout the time course (Fig. 10A) and that of initial PC of the *act1 lpcat1 lpcat2* line  
460 (Fig. 7D, 10B), but not similar to the labeled PC which remains near the end of the time  
461 course in both lines (Fig. 10B).

462

## 463 **DISCUSSION**

464

465 Biochemical, genetic, and molecular biology research on plant membrane lipid  
466 assembly over the past 40 years has indicated a complicated metabolic network of  
467 reactions (Fig. 1) that requires the trafficking of intermediates between multiple  
468 subcellular compartments to produce the diverse molecular species of lipids crucial to  
469 cellular function. While many of the acyltransferases and desaturases involved in lipid  
470 assembly have been identified the pathways of acyl trafficking, the identity of lipid  
471 intermediates, and the trafficking proteins involved in the eukaryotic pathway have  
472 remained more elusive. Major advances over the past 15 years include the identification  
473 of a free fatty acid transporter for export of nascent fatty acids from the plastid (Li et al.,  
474 2015), the determination that nascent fatty acids exported from the chloroplast in leaves  
475 are predominantly first incorporated into PC by an LPCAT-type reaction of acyl editing  
476 rather than the initial attachment to G3P through *de novo* glycerolipid assembly (Bates  
477 et al., 2007), and the characterization of a protein complex involved in the transport of  
478 the eukaryotic pathway assembled lipid intermediate into the plastid for galactolipid  
479 production (Xu et al., 2005). However, the exact lipid species transported from the ER to  
480 the chloroplast has remained unclear; DAG, PA, PC and LPC have all been suggested.

481 Eukaryotic pathway-derived lipids are characterized by 18-carbon fatty acids at the *sn*-2  
482 position, while the *sn*-2 acyltransferases of the prokaryotic pathway in the plastid utilize  
483 16-carbon fatty acids. If LPC is transported to the outer membrane of the plastid it must  
484 be acylated to PC by an LPCAT activity prior to turnover to DAG or PA to produce the  
485 correct molecular species of the eukaryotic pathway. Since LPCAT activity has been  
486 implicated in both the trafficking of fatty acids from the chloroplast to the ER in seeds  
487 (Bates et al., 2012) and from the ER to the chloroplast in leaves (Mongrand et al., 1997;  
488 Moreau et al., 1998; Mongrand et al., 2000), we sought to gain a better understanding  
489 of the roles of LPCAT1 and LPCAT2 in leaf acyl trafficking by analyzing the lipid  
490 accumulation and acyl fluxes within the *act1 lpcat1 lpcat2* mutant background.

491

492 **LPCAT1 and LPCAT2 encode chloroplast-localized LPCATs that are involved in**  
493 **the direct incorporation of newly synthesized fatty acids into PC through acyl**  
494 **editing**

495

496 The rapid incorporation of nascent fatty acids into predominantly the *sn*-2  
497 position of PC through acyl editing, rather than through *de novo* glycerolipid synthesis,  
498 was originally characterized in developing pea leaves, an 18:3 plant (Bates et al., 2007).  
499 In this study the *act1* mutation (Kunst et al., 1988) was utilized to essentially convert  
500 *Arabidopsis* into an 18:3 plant. Here we demonstrate that in *act1* leaves nascent fatty  
501 acids are also predominantly incorporated initially into the *sn*-2 position of PC,  
502 consistent with a highly active PC acyl-editing cycle in *Arabidopsis* leaves (Fig. 5B, 6A,  
503 7C). When LPCAT1 and LPCAT2 were additionally mutated in the *act1 lpcat1 lpcat2*  
504 line, the chloroplast-associated LPCAT activity was reduced at least 85% (Fig. 4), the  
505 initial incorporation of nascent fatty acids into PC was reduced concomitantly with an  
506 increase into DAG (Fig. 6A-B), and the stereochemistry of incorporation into PC was  
507 completely switched to favor *sn*-1 in a proportion similar to the rapidly synthesized *de*  
508 *novo* DAG (Fig. 7B,D). These results suggest that without chloroplast-associated  
509 LPCAT1 and LPCAT2 activity the newly synthesized fatty acids are rerouted to enter  
510 PC through the GPAT and LPAT reactions of *de novo* glycerolipid synthesis rather than  
511 LPCAT-based acyl editing in leaves (Fig. 11). It is not clear if the residual ~15% of wild-

512 type LPCAT activity measured in the *act1 lpcat1 lpcat2* isolated chloroplasts is due to  
513 other chloroplast-associated lysophospholipid acyltransferases (LPLAT) (Larsson et al.,  
514 2007; Stalberg et al., 2009; Bulat and Garrett, 2011; Jasieniecka-Gazarkiewicz et al.,  
515 2016), or due to partial contamination of the isolated chloroplasts with other cellular  
516 membrane fractions containing LPLATs (Larsson et al., 2007; Tjellström et al., 2012).  
517 However, the complete switch in the *in vivo*-labeled PC stereochemistry suggests that  
518 any other putative chloroplast-associated LPLATs do not compensate for the lack of  
519 LPCAT1 and LPCAT2 in the direct flux of nascent fatty acids into PC through acyl  
520 editing.

521

## 522 **Roles of PC acyl editing in leaves**

523

524 Here we demonstrate a role for LPCAT1 and LPCAT2 in the direct incorporation  
525 of newly synthesized fatty acids into PC as they exit the chloroplast in leaves and show  
526 that this role is dispensable in the *lpcat1 lpcat2* background (Fig. 11A-B). However, the  
527 role of LPCAT1 and LPCAT2 in leaves likely extends beyond trafficking of nascent fatty  
528 acids to PC. PC is the site of ER-localized fatty acid desaturation (Li-Beisson et al.,  
529 2013). Previously, LPCAT1 and LPCAT2 were demonstrated to be involved in acyl flux  
530 through PC to provide polyunsaturated fatty acids (PUFA) for seed triacylglycerol  
531 biosynthesis (Bates et al., 2012; Wang et al., 2012a). Acyl flux through PC for PUFA  
532 production is likely also a key role for acyl editing in leaves. Recent work has indicated  
533 that the amount of PUFA that accumulate in ER lipids is related to both desaturase  
534 activity and the rate of acyl flux through PC. When acyl flux slows down, more PUFA  
535 accumulate due to enhanced residence time on PC for desaturation (Maatta et al.,  
536 2012; Meï et al., 2015; Botella et al., 2016). While young leaves are expanding, acyl flux  
537 through PC is high for membrane lipid production, and little change in PC fatty acid  
538 composition was observed in the *act1 lpcat1 lpcat2* mutant (Fig. 3A). However, as  
539 leaves matured, more 18:2 and 18:3 and less 18:1 accumulated in PC as compared to  
540 *act1* (Fig. 3B,C), and a similar change was observed in PE (Fig. 3F). This result  
541 suggests that LPCAT1- and LPCAT2-based acyl editing has homeostatic roles likely  
542 involving distribution of PUFA to other lipids across the leaf life cycle. In the *lpcat1*

543 *lpcat2* mutant background, the plant may compensate for the loss of acyl editing by  
544 increasing other mechanisms of acyl flux through PC as indicated in seeds (Bates et al.,  
545 2012; Wang et al., 2012a), or providing PUFA from chloroplast sources. Recently, a PG  
546 lipase was implicated in the export of PUFA from the chloroplast for seed oil  
547 biosynthesis (Wang et al., 2017; Aulakh and Durrett, 2019). The only lipid with a change  
548 in abundance in the *act1 lpcat1 lpcat2* line was PG (Fig. 2C). It is possible that the loss  
549 of LPCAT1- and LPCAT2-based acyl editing has activated this or other mechanisms of  
550 chloroplast-to-ER trafficking of PUFA. However, the *in vivo* metabolic labeling  
551 experiments (Fig. 6, 8) did not measure a significant difference in PG labeling,  
552 suggesting acyl flux through PG may be a minor contribution to ER PUFA content.

553 The only lipid that had significant differences in [<sup>14</sup>C]fatty acid accumulation  
554 between lines across the pulse-chase time course was TAG (Fig. 8F). The *act1 lpcat1*  
555 *lpcat2* line accumulated less labeled TAG than did the *act1* line. TAG does not  
556 accumulate to high mass levels in leaves, but a small metabolically-active pool that is  
557 constantly synthesized and turned over is believed to act as a free fatty acid buffer  
558 during times of high rates of fatty acid synthesis or stress (Xu and Shanklin, 2016).  
559 Recently, phospholipid:diacylglycerol acyltransferase (PDAT) was demonstrated to be a  
560 key part of TAG production in *Arabidopsis* leaves (Fan et al., 2013a; Fan et al., 2013b;  
561 Fan et al., 2014). PDAT transfers a fatty acid from the *sn*-2 position of PC to DAG,  
562 producing TAG and LPC. LPCAT works in tandem with PDAT to regenerate PC from  
563 the co-produced LPC (Xu et al., 2012). Together, PDAT and LPCAT could lead to  
564 channeling of nascent fatty acids exported from the plastid into PC and then TAG during  
565 high rates of fatty acid synthesis. The reduced TAG labeling in the *act1 lpcat1 lpcat2*  
566 mutant is likely due to inefficient PDAT activity without an LPCAT to regenerate the PC  
567 substrate. Together, these results suggest a variety of possible roles for LPCAT1- and  
568 LPCAT2-based acyl editing in leaves.

569

## 570 **MGDG production from PC is independent of LPCAT1 and LPCAT2**

571

572 LPCAT activity has been implicated in the acylation of LPC transported from the  
573 ER to the chloroplast as part of eukaryotic pathway trafficking of substrates for MGDG

synthesis. This previous conclusion originally came from *in vitro* experiments demonstrating the transfer of LPC from isolated microsomes to isolated chloroplasts from leek seedlings, and its acylation to PC by the chloroplast-associated LPCAT activity (Bessoule et al., 1995). Further *in vivo* metabolic labeling pulse-chase experiments in leek seedlings demonstrated that PC containing predominantly *sn*-2 labeled fatty acids gave rise to MGDG labeled mostly at *sn*-1 (Mongrand et al., 1997; Mongrand et al., 2000). The conclusion was that only the *sn*-1 fatty acid was transferred to the chloroplast and, combined with the previous *in vitro* experiments, suggested that LPC was the molecule transferred from the ER to the chloroplast.

The *act1* mutation eliminates the prokaryotic pathway of MGDG synthesis. When this mutant was crossed with the *tgd1-1* mutant (a part of the OEM to IEM transporter that provides substrate for chloroplast lipid synthesis) no viable double mutants were recovered (Xu et al., 2005), indicating that disruptions of the eukaryotic pathway in the *act1* background are lethal. However, we demonstrate that the *act1 lpcat1 lpcat2* triple mutation causes at least an 85% reduction in chloroplast LPCAT activity (Fig. 4), little to no growth alteration (Supplemental Fig. 2), and no effect on the accumulation of galactolipids (Fig. 2). Therefore, we conclude that LPCAT1 and LPCAT2, and LPC trafficking are not a key part of eukaryotic pathway galactolipid synthesis. However, we cannot rule out that the residual ~15% of wild-type LPLAT activity associated with isolated *act1 lpcat1 lpcat2* chloroplasts may represent a minimal flow of LPC transported from the ER for other purposes, such as incorporation of PC into the outer leaflet of the chloroplast OEM. If this minimal flow of LPC occurs, the formation of PC must be through a LPLAT other than LPCAT1 and LPCAT2.

To gain a better understanding of the mechanisms involved in the PC–MGDG precursor–product relationship we performed a long term [<sup>14</sup>C]acetate pulse-chase experiment. The *act1* mutant and *act1 lpcat1 lpcat2* triple mutant showed little difference in quantitative turnover of initially-labeled PC or in the subsequent incorporation of the labeled fatty acids into MGDG (Fig. 8). In addition, the labeled fatty acid composition of DAG, PC, and MGDG was the same between the two lines across the pulse-chase time course (Fig. 9). These results further suggest that the *lpcat1 lpcat2* mutation does not affect the ER-to-chloroplast trafficking of the eukaryotic pathway. When the

605 stereochemistry of labeled fatty acids in PC and MGDG of *act1* were analyzed, we  
606 found a similar result to that of the leek seedlings (Mongrand et al., 2000) where PC  
607 was mostly *sn*-2 labeled and the labeled MGDG that accumulated from turnover of PC  
608 was mostly *sn*-1 labeled (Fig. 10). From the *act1* labeling data alone (in an essentially  
609 18:3 plant, similar to leek), the transfer of LPC would make sense. However, the  
610 stereochemical analysis of DAG, PC, and MGDG of the *act1 lpcat1 lpcat2* line revealed  
611 a different underlying mechanism.

612 In both the short continuously labeling time course and at the end of the pulse  
613 (time 0), the stereochemistry of DAG and PC from *act1 lpcat1 lpcat2* were very similar,  
614 with more nascent labeled fatty acids at *sn*-1 than *sn*-2 (Fig. 7, 10). Therefore, the lack  
615 of LPCAT1- and LPCAT2-based acyl editing leads to nascent fatty acid incorporation  
616 into PC though eukaryotic *de novo* glycerolipid assembly, which dictates the  
617 stereochemical distribution of fatty acids in DAG and PC. The labeled fatty acid  
618 stereochemical distribution that accumulates in MGDG over time in both lines (Fig. 10C)  
619 is also very similar to the *de novo* synthesized DAG and PC (Fig. 10A-B). Therefore, we  
620 conclude that the DAG backbone utilized to synthesize eukaryotic MGDG is derived  
621 from a PC pool produced from *de novo* eukaryotic glycerolipid assembly and is distinct  
622 from the pool of PC undergoing LPCAT1- and LPCAT2-based acyl editing.

623 Figure 11 incorporates the [<sup>14</sup>C]acetate pulse-chase data onto new models of  
624 eukaryotic pathway acyl flux that demonstrate the metabolically distinct pools of PC  
625 involved in acyl editing and eukaryotic pathway MGDG production. When LPCAT1 and  
626 LPCAT2 are present in *act1* the labeling of PC is dominated by the rapid *sn*-2 acyl  
627 editing (Fig. 11A). Acyl editing is a constant exchange of acyl groups in PC with the  
628 acyl-CoA pool, and it allows the PUFA produced on PC to be utilized by the GPAT and  
629 LPAT reactions of the eukaryotic pathway (Bates et al., 2007; Bates et al., 2009; Bates  
630 et al., 2012; Bates, 2016). Therefore, during the pulse-chase the labeled acyl groups  
631 can leave PC by acyl editing and are assembled into DAG with more *sn*-1 labeling than  
632 *sn*-2, which is then used for PC synthesis. If this *de novo* synthesized pool of PC is  
633 rapidly turned over to produce the substrate for MGDG synthesis, MGDG will have the  
634 same *sn*-1-labeled stereochemistry, and it would not have much effect on the  
635 stereochemistry of “total labeled PC”, which is dominated by the separate highly-labeled

636 acyl-editing PC pool. It is only when LPCAT activity is removed in the *act1 lpcat1 lpcat2*  
637 triple mutant that the flux through *de novo* PC to MGDG can be measured separately  
638 from the acyl-edited PC pool (Fig. 10), which reveals a clear PC–MGDG precursor–  
639 product relationship (Fig. 11B–C). Therefore, the glycerol backbone and both fatty acids  
640 (derived mostly from PC acyl editing) that are assembled onto *de novo* PC are  
641 ultimately the “DAG backbone” utilized for chloroplast MGDG synthesis. This model is  
642 also supported by recent characterization of an unusual Δ6 desaturated fatty acid  
643 produced transgenically in Arabidopsis leaves at only the *sn*-2 position of PC. However,  
644 the Δ6D fatty acid was redistributed approximately equally to the *sn*-1 and *sn*-2  
645 positions of MGDG (Hurlock et al., 2018). Removal of the Δ6D fatty acid from PC by  
646 acyl editing (Fig. 11A) and its subsequent incorporation into both positions of *de novo*  
647 DAG by GPAT/LPAT activities of the eukaryotic pathway prior to MGDG synthesis is  
648 consistent with our new model of acyl flux.

649

#### 650 **Changes to eukaryotic pathway acyl flux within the *act1 lpcat1 lpcat2* background**

651

652 In wild-type and *act1* leaves, the PC acyl-editing cycle may occur by at least  
653 three mechanisms (Bates, 2016): (1) both the forward and reverse reactions of LPCAT  
654 (Lager et al., 2013; Jasieniecka-Gazarkiewicz et al., 2016); (2) a phospholipase A<sub>2</sub>  
655 (PLA<sub>2</sub>) hydrolysis of PC to LPC and a free fatty acid (FFA), FFA activation to acyl-CoA  
656 by LACS, and LPC conversion to PC by the forward LPCAT reaction using a different  
657 acyl-CoA (also known as the Lands Cycle (Lands, 1965)); (3) either mechanism 1 or 2  
658 plus a LPC:LPC transacylase (LPCT) (Lager et al., 2015) and a glycerophosphocholine  
659 acyltransferase (GPCAT) (Lager et al., 2015; Glab et al., 2016). LPCT transfers an acyl  
660 group from one LPC to another producing PC and glycerophosphocholine, which is then  
661 converted back to PC by the combined action of GPCAT and LPCAT. In relation to the  
662 multiple possible enzymatic mechanisms for acyl editing, two important details from the  
663 [<sup>14</sup>C]acetate pulse-chase experiment must be pointed out. (1) In both *act1* and *act1*  
664 *lpcat1 lpcat2*, DAG has approximately 30% <sup>14</sup>C-PUFA at the end of the pulse (time 0  
665 chase), indicating newly synthesized 18:1 is rapidly incorporated into PC for  
666 desaturation, and then incorporated into DAG. (2) The *act1 lpcat1 lpcat2* PC

667 stereochemical labeling within the pulse-chase experiment switches from more *sn*-1  
668 label at time 0 to more *sn*-2 label at the end of the time course. Based on the  
669 mechanisms of acyl editing, multiple possible scenarios could explain both the *act1*  
670 *lpcat1 lpcat2* DAG PUFA content and the stereochemistry switch in PC (Fig. 11B-C).

671 First, in model Fig. 11B the *lpcat1 lpcat2* mutation eliminates acyl chain removal  
672 from PC by acyl editing (e.g. eliminating acyl-editing mechanism 1). Therefore, the  
673 PUFA-labeled DAG represents PC-derived DAG after desaturation. In model 11B, the  
674 switch in labeled PC stereochemistry may be through selective molecular species  
675 trafficking. Not all PC that is synthesized *de novo* is turned over for chloroplast lipid  
676 synthesis. Some PC has a structural role within various cellular endomembrane  
677 systems. It is possible that the turnover of mostly *sn*-1 labeled molecular species for  
678 chloroplast lipid synthesis has left behind a majority of molecular species that contain  
679 *sn*-2 labeled fatty acids.

680 Second, the *lpcat1 lpcat2* mutation eliminates the LPCAT portion of a Lands  
681 Cycle, but not the continual generation of LPC by PLA<sub>2</sub>. In model Fig. 11C red and blue  
682 arrows only, PLA<sub>1</sub>- or PLAB-based turnover of LPC generated by the PLA<sub>2</sub> would  
683 completely remove the fatty acids from PC leading to complete PC turnover.  
684 Considering PC is also undergoing desaturation (Fig. 9), the [<sup>14</sup>C]18:1 originally  
685 incorporated into PC will be converted to [<sup>14</sup>C]18:2 and [<sup>14</sup>C]18:3 over time. When these  
686 fatty acids are removed and then reutilized for *de novo* glycerolipid synthesis it will  
687 produce *de novo* DAG containing PUFA, and the labeled fatty acid stereochemistry in  
688 PC will then be determined by the acyl selectivity of GPAT/LPAT. This will lead to  
689 different labeled stereochemical molecular species of PC produced from the <sup>14</sup>C-PUFA  
690 and newly synthesized <sup>12</sup>C-18:1 during the chase. In support this hypothesis, increased  
691 expression of various lipases with as-yet uncharacterized functions were measured in  
692 developing seeds of the *lpcat1 lpcat2* mutant, suggesting the possibility of a modified  
693 method to remove PUFA from PC in the *lpcat1 lpcat2* background (Wang et al., 2012a).

694 Third (model Fig. 11C, all arrows), PLA<sub>2</sub> activity in *act1 lpcat1 lpcat2* would  
695 produce LPC, which could be converted back to PC by LPCT (as in acyl-editing  
696 mechanism 3). This type of reaction would transfer an *sn*-1 acyl group from one LPC to  
697 a second LPC and thus could move a labeled fatty acid from the *sn*-1 to *sn*-2 position in

698 PC. The GPC also produced can be reacylated to LPC by GPCAT, and thus could  
699 produce a cycle of *sn*-1/*sn*-2 acyl switching within the *lpcat1 lpcat2* background. From  
700 the current experiments it is not clear which of these three possibilities may be  
701 occurring, but it is likely that a pool of PC that remains in the ER (model 1, Fig. 11B)  
702 may be undergoing acyl turnover (models 2/3, Fig. 11C), which leads to a different  
703 stereochemistry of the labeled fatty acids in PC over time (Fig. 10B).

704

705 **Current model for leaf glycerolipid synthesis and trafficking in wild-type**  
706 ***Arabidopsis* leaves**

707

708 Figure 12 is a modification of Fig. 1 based on our current results and displays the  
709 current areas of uncertainty in the eukaryotic pathway of leaf glycerolipid synthesis. The  
710 model no longer indicates that LPC can be transferred from the ER to the chloroplast for  
711 galactolipid production. It also has three metabolically distinct pools of PC. PC(1) is  
712 involved in LPCAT1- and LPCAT2-based acyl editing and may be located at the  
713 chloroplast surface or a ER-chloroplast membrane contact site. A membrane contact  
714 site might make the most sense because it would allow PC containing newly  
715 synthesized 18:1 to diffuse through the ER to the FAD2 and FAD3 enzymes for  
716 desaturation. PC(2) is the pool that is produced by *de novo* PC synthesis within the  
717 eukaryotic pathway; it is a substrate for desaturases and provides PC that migrates  
718 through the ER to other locations. PC(3) is the pool that is turned over to produce the  
719 substrate for MGDG synthesis, and it may have been further desaturated by FAD2 and  
720 FAD3 than PC(2). In addition, the exact PC(3)-derived intermediate (DAG or PA)  
721 transported to the IEM by the TGD1-5 complex is still unclear. The location of PC(3)  
722 turnover is also unclear; it could be the ER, the chloroplast surface, or a ER-chloroplast  
723 membrane contact site. Recent characterization of the ALA10 flipase mutant suggest  
724 the likely involvement of a membrane contact site for ER-to-chloroplast trafficking  
725 (Botella et al., 2016). Considering the multiple possible roles for membrane contact sites  
726 in acyl trafficking, it may be plausible that there are ER-chloroplast contact sites with  
727 specific functions in acyl export from the chloroplast involving LPCAT1- and LPCAT2-

728 based acyl editing and separate contact sites with specific function in eukaryotic lipid  
729 import into the chloroplast for galactolipid production.

730 The findings presented here strongly enhance our understanding of eukaryotic  
731 pathway of membrane lipid production in leaves by demonstrating that (1) *LPCAT1* and  
732 *LPCAT2* encode the major chloroplast-associated LPCAT activities; (2) the major role of  
733 *LPCAT1* and *LPCAT2* is for direct incorporation of newly synthesized fatty acids into PC  
734 through acyl editing as the fatty acids are transported out of the chloroplast; (3) *LPCAT1*  
735 and *LPCAT2* activity is not involved in the transfer of LPC from the ER to the chloroplast  
736 within eukaryotic pathway galactolipid production; (4) the PC–MGDG precursor–product  
737 relationship of acyl flux involves removal of acyl chains from PC by acyl editing prior to  
738 *de novo* PC synthesis and the subsequent turnover of PC for MGDG production; and (5)  
739 PC acyl editing and PC turnover for MGDG production involve metabolically distinct  
740 pools of PC. This last result suggests that an underlying spatial organization of distinct  
741 PC metabolism may be a key part of the efficient acyl trafficking through the eukaryotic  
742 pathway. While there is still uncertainty regarding which PC-derived lipid is trafficked  
743 from the ER to the chloroplast, the *Arabidopsis act1 lpcat1 lpcat2* line characterized  
744 here may be particularly useful for future studies because it allows for metabolic tracing  
745 of the PC–MGDG precursor–product relationship without the complications of acyl flux  
746 around the PC acyl-editing cycle.

747

## 748 METHODS

749

### 750 Plant materials

751 *Arabidopsis thaliana* lines used in this study include: wild-type Columbia-0 (Col-0), *act1*  
752 mutant (ACT1, At1G32200; Kunst et al., 1988), *lpcat1 lpcat2* double mutant (LPCAT1,  
753 AT1G12640; LPCAT2, AT1G63050; Bates et al., 2012), and the *act1 lpcat1 lpcat2* triple  
754 mutant generated here.

755

### 756 Plant germination and growth

757 Seeds were sterilized in aqueous 10% bleach, 27% ethanol, and 0.1% SDS,  
758 rinsed with water 5 times and applied to germination plates (1x MS salts, 0.05% MES

759 free acid, 1% sucrose, and 0.8% Agar, pH 5.7) in a 0.1% agar solution. The plates were  
760 incubated at 4 °C for 3 days, then placed in a growth chamber under ~150 µmol  
761 photons m<sup>-2</sup> s<sup>-1</sup> white light using 14 h/10 h day/night cycle at 23 °C constant temperature  
762 until all lines germinated and produced two true leaves (approximately 7-10 days). The  
763 seedlings were then transferred to soil and placed back into the growth chambers. All  
764 plants were watered 3 times a week with on watering consisting of Peter's NPK 20-20-  
765 20 (0.957g/l) fertilizer solution. During the crossing and harvest of seeds, the plants  
766 were grown at the same growth condition but with constant light.

767

#### 768 **Production of *act1* *lpcat1* *lpcat2* triple mutant**

769 The *act1* and *lpcat1* *lpcat2* were crossed via cross-pollination by hand. The  
770 screening of *act1* was done by identifying absence of hexadecatrienoic acid (16:3) in  
771 whole leaf FAME by gas chromatography. The screening of *lpcat1* *lpcat2* was done by  
772 PCR of leaf tissue with previously described primers (Bates et al., 2012; Xu et al.,  
773 2012). With the Phire Plant Direct PCR Mastermix (Thermo Scientific) as per the  
774 manufacturer's instructions.

775

#### 776 **Production of FAME and gas chromatography**

777 Plant tissue and collected lipid samples were converted to fatty acid methyl  
778 esters (FAME) with an internal 17:0 TAG standard by heating to 85 °C for 1.5 h in 5%  
779 sulfuric acid in methanol. After forcing a phase separation by adding hexane and 0.88%  
780 potassium chloride, the hexane phase containing the FAME was analyzed by gas  
781 chromatography with flame ionization detection on a Shimadzu GC-2010 with a  
782 RESTEK Rtx®-65 column (30m, 0.25mm ID, df = 0.25 µm), with method run parameters  
783 of 190 °C prior for 2 min, and then the temperature increased to 270 °C at 10 °C/min  
784 and held at 270 °C for 2 min. The detector was set at 275 °C.

785

#### 786 **Lipid extraction**

787 The lipid extraction is based off of Hara and Radin (1978). Plant tissues were  
788 quenched in 80-85 °C isopropanol with 0.01% butylated hydroxytoluene for 10 min. The  
789 tissue was homogenized with polytron and moved to new glass tubes. The polytron was

washed with isopropanol and hexane to recover all remaining sample and combined with the ground tissue to a final proportion of hexane/isopropanol/water of 6/4/0.2 (v/v/v). The polytron was washed further between samples to avoid cross-contamination. Lipids were collected into the hexane phase by adding half of the sample volume of 6.6% sodium sulfate. The aqueous phase was back extracted using hexane/isopropanol (7/2) and combined with the previous hexane extract. The combined organic sample was dried down under nitrogen and resuspended in known volume of toluene. For radiolabeled samples, the lipids were resuspended in chloroform/methanol (2:1) and subjected to a second phase separation by the addition of 0.88% potassium chloride to remove any excess radiolabel. The organic phase was collected, dried down in nitrogen, and resuspended in known volume of toluene. Chlorophyll was measured as in Arnon (1949). Each replicate was a separate extraction of enough leaf material from many plants to make approximately 0.3 g fresh weight.

803

#### 804 **Chloroplast isolation and LPCAT assays**

Arabidopsis lines were grown on soil in a growth chamber set to 12/12-h day/night cycle, 25°C, and 150  $\mu$ mol photons  $m^{-2} s^{-1}$  light. 25 grams of leaf tissue was harvested at 36 days (Col-0, *lpcat1 lpcat2*) and 44 days (*act1, act1 lpcat1 lpcat2*) after 16 hours of dark treatment. Chloroplast isolation was as described by (Kubis et al., 2008), with a modified concentration of 0.33 M sorbitol (instead of 0.3 M) for the isolation and resuspension buffers. The chlorophyll content of isolated chloroplasts was measured as in Arnon (1949) with a Thermo Scientific Genesys 50 UV-Vis spectrophotometer.

LPCAT assays were performed on chloroplasts equivalent to 150  $\mu$ g chlorophyll, in 0.3 mL in a 1.5-mL tube containing 1 mM soy LPC, and 13.6  $\mu$ M [ $^{14}$ C]oleoyl-CoA 55 mCi/mmol (American Radiolabeled Chemicals, Inc.), at 30 °C, with 300 rpm mixing for 30 minutes on an Eppendorf Thermomixer. The reaction was stopped by adding 1.2 mL CHCl<sub>3</sub>/MeOH/Formic Acid (2/1/1, v/v/v) and vigorous vortexing. The assay mixture was transferred to 8 mL glass tubes and the assay vessel was washed once with a second aliquot of CHCl<sub>3</sub>/MeOH/formic acid, then combined with the previous extract. Addition of 0.3 mL KCl to the mixture and centrifugation at 2000 g produced phase separation,

821 and the lower organic phase was removed to a new 8 mL glass tube. The aqueous  
822 phase was washed with 1 mL of CHCl<sub>3</sub> and combined with previous organic phase.  
823 The CHCl<sub>3</sub> extract was evaporated under a stream of N<sub>2</sub> and resuspended in 100  $\mu$ L  
824 CHCl<sub>3</sub>. Two aliquots of 5  $\mu$ L were dissolved in 5 mL Eco-Scint liquid scintillation cocktail  
825 (National Diagnostics) and radioactivity measured with a Packard 2200CA Liquid  
826 Scintillation Counter to quantify the radioactivity in the whole extract. The remaining  
827 extract was loaded onto Millipore-Sigma Silica gel 60 TLC plates in 1 cm bands with  
828 non-radioactive lipid standards in adjacent lanes. The TLC plate was developed in  
829 CHCl<sub>3</sub>/MeOH/acetic acid/acetone/water (35/25/4/14/2, v/v/v/v/v). After development, the  
830 TLC plate was air dried and stained with iodine vapor for visualization of lipid mass  
831 bands, and the standards were marked with a radioactive dot. The TLC plate was  
832 placed against phosphor imaging screen for 24 hours and developed by a GE Typhoon  
833 FLA 7000 phosphor imager. Identification of radioactive lipids from the assays was  
834 based on comigration with lipid standards. Relative quantification of all radioactive  
835 bands was by ImageQuant software version 7.0.

836

#### 837 ***In vivo* [<sup>14</sup>C]acetate metabolic labeling**

838 For both continuous and pulse-chase labeling 3-week-old plant tissue was  
839 floated on incubation medium consisting of 20 mM MES, 0.1X MS salts, and 0.01%  
840 Tween 20 at pH 5.5, in a shaking water bath at 23 °C under ~150  $\mu$ mol photons m<sup>-2</sup> s<sup>-1</sup>  
841 white light.

842 For the continuous labeling, leaves were harvested into the incubation media and  
843 placed in the shaking water bath to equilibrate temperature. To start the time course the  
844 medium was removed and replaced with incubation medium containing 0.255 mM [1-  
845 <sup>14</sup>C]acetate sodium salt 55 mCi/mmol (American Radiolabeled Chemicals Inc.) at 12.75  
846  $\mu$ Ci/ml. The leaves were incubated for different timepoints (5, 10, 15, and 60 minutes)  
847 after which they were removed from the medium and quenched in isopropanol with  
848 0.01% BHT at 85 °C prior to lipid extraction. Fifteen leaves were used per time point  
849 replicate. The labeled medium was reused between different timepoints of same  
850 replicate/plant line. Each timepoint was harvested/radiolabeled separately in replicates  
851 of three per plant line.

852 For the pulse-chase labeling, whole rosettes were harvested by removing the  
853 roots, and immediately placed into the incubation medium. Once rosettes for all  
854 timepoints for each replicate/plant line were collected, the incubation medium was  
855 removed and replaced with medium containing 0.153 mM [<sup>14</sup>C]acetate at 7.65  $\mu$ Ci/ml.  
856 After 15 mins of pulse, the radiolabeled medium was removed, and the tissues were  
857 washed 5 times using incubation medium. The 0-timepoint was immediately collected  
858 and the remaining rosettes were incubated in incubation medium for 1, 4, 22, 28, and 51  
859 hours. The collected tissues were quenched in isopropanol with 0.01% BHT at 85 °C  
860 prior to lipid extraction. Three to four whole rosettes were used per time point replicate.  
861 Three replicate pulse-chase time courses were carried out per line, and the radiolabeled  
862 medium for the pulse was reused for the three replicates within each line.

863 Analysis of radioactivity of extracts in disintegrations per minute (DPM) by liquid  
864 scintillation counting in EcoScint Original scintillation fluid (National Diagnostics) was on  
865 a Beckman Coulter LS 6500 liquid scintillation counter. Relative radioactivity of lipids  
866 separated on TLC plates was measured using phosphor imaging on a GE Typhoon  
867 FLA7000, and ImageQuant analysis software.

868

#### 869 **Glycerolipid and FAME separations by TLC**

870 Polar lipids were separated using thin layer chromatography (TLC) plates (20 x  
871 20 cm Analtech Silica gel HL 250  $\mu$ M thickness) pre-treated with 0.15 M ammonium  
872 sulfate and baked at 120 °C for 3 hours. Less than 250  $\mu$ g lipid was loaded per cm and  
873 separated in toluene/acetone/water (30/91/7, v/v/v). Neutral lipids were loaded directly  
874 onto the untreated EMD Millipore silica gel 60 20 x 20 cm TLC plates and separated in  
875 hexane/ether/acetic acid (70/30/1, v/v/v). FAME were loaded onto EMD Millipore plates  
876 treated in 7.5% silver nitrate in acetonitrile and baked at 100 °C for 5 minutes prior to  
877 use. The FAME were first separated to 75% of plate height in hexane/ether (1/1, v/v),  
878 then fully developed in hexane/ether (9/1, v/v).

879

#### 880 **Stereochemical Analysis of <sup>14</sup>C labeled lipids**

881 Lipids were separated by TLC, stained with 0.005% primulin in acetone/water  
882 (4/1, v/v) and visualized under UV light. Polar lipids were eluted from silica gel with

883 chloroform/methanol/water (5/5/1, v/v/v), and the chloroform phase was collected after  
884 phase partitioning with 0.88% KCl. Neutral lipids were eluted from silica gel with  
885 chloroform/methanol (9/1, v/v). All lipids were dried under nitrogen prior to being  
886 suspended in diethyl ether for lipase digestion.

887 Stereochemical analysis of DAG and MGDG was done by enzymatic digest with  
888 lipase from *Rhizomucor miehei* (Sigma). Buffer consisting of 50 mM boric acid and 5  
889 mM calcium chloride at 7.8 pH and the lipase were added at 4:1 ratio for diacylglycerol  
890 (DAG) and 39:1 ratio for MGDG. The reaction was carried out for 15 minutes for both  
891 DAG and MGDG with a goal of 50% to 60% and 20% to 30% digestion respectively.  
892 The reaction was stopped by adding chloroform/methanol (1:1), the chloroform phase  
893 was collected for TLC. The digested lipids were separated using hexane/diethyl  
894 ether/acetic acid (35/70/1.5, v/v/v) for DAG and acetone/toluene/water (91/30/7.5, v/v/v)  
895 for MGDG on non-treated silica TLC plates.

896 Stereochemical analysis of PC was done with Phospholipase A<sub>2</sub> from bee venom  
897 (*Apis mellifera*) (Sigma). Buffer containing 50 mM Tris-HCl and 5 mM calcium chloride  
898 at 8.7 pH and PLA<sub>2</sub> were added such that the enzyme was about 0.25 units. The  
899 reaction was carried out for 5 minutes and the reaction mixture was dried down under  
900 nitrogen. The digested lipids were extracted by adding chloroform/methanol/0.15 M  
901 acetic acid (38/19/15, v/v/v) and collecting the organic phase. The lipids extracted were  
902 separated using chloroform/methanol/acetic acid/water (50/30/8/4, v/v/v/v) on silica TLC  
903 plates.

904

## 905 **Data analysis**

906 All calculations from raw data were done in Microsoft Excel. Graphing and  
907 statistical analysis done with GraphPad Prism version 7.04.

908

## 909 **Accession Numbers**

910 *LPCAT1* (At1g12640), *LPCAT2* (At1g63050), *ACT1/ATS1* (At1g32200)

911

## 912 **Supplemental Data**

913 **Supplemental Figure 1.** Relative gene expression of LPCAT1, LPCAT2, LPEAT1,  
914 LPEAT2 in leaves and seeds of wild-type Arabidopsis.

915 **Supplemental Figure 2.** Pictures of growth of Col-0, *act1*, *lpcat1 lpcat2*, and *act1*  
916 *lpcat1 lpcat2*.

917 **Supplemental Figure 3.** Lipid fatty acid composition at 2 weeks.

918 **Supplemental Figure 4.** Lipid fatty acid composition at 3 weeks.

919 **Supplemental Figure 5.** Lipid fatty acid composition at 4 weeks.

920

921 **Acknowledgements**

922 We thank Dr. Jay Shockey for critical reading of the manuscript and helpful  
923 discussions. This work was supported by the National Science Foundation Grant No.  
924 1930559, and by the Agriculture and Food Research Initiative Grant No. 2017-67013-  
925 29481 and No. 2017-67013-26156 from the USDA National Institute of Food and  
926 Agriculture. In addition, this work utilized Mississippi INBRE facilities funded by the  
927 National Institutes of Health under grant number P20GM103476.

928

929 **Author Contributions**

930 NK, BSJ, and PDB designed the research; performed research; analyzed data; and  
931 wrote the paper.

932

933 **References**

934

935 **Allen, D.K., Bates, P.D., and Tjellström, H.** (2015). Tracking the metabolic pulse of  
936 plant lipid production with isotopic labeling and flux analyses: Past, present and  
937 future. *Prog. Lipid Res.* **58**, 97-120.

938 **Andersson, M., and Dörmann, P.** (2008). Chloroplast Membrane Lipid Biosynthesis  
939 and Transport. *The Chloroplast: Interactions with the Environment* **13**, 125.

940 **Andersson, M.X., Goksor, M., and Sandelius, A.S.** (2007). Optical manipulation  
941 reveals strong attracting forces at membrane contact sites between endoplasmic  
942 reticulum and chloroplasts. *J Biol Chem* **282**, 1170-1174.

943 **Arnon, D.I.** (1949). Copper enzymes in isolated chloroplasts - polyphenoloxidase in  
944 Beta-Vulgaris. *Plant Physiol.* **24**, 1-15.

945 **Arondel, V., Lemieux, B., Hwang, I., Gibson, S., Goodman, H.M., and Somerville,**  
946 **C.R.** (1992). Map-based cloning of a gene controlling omega-3-fatty-acid  
947 desaturation in *Arabidopsis*. *Science* **258**, 1353-1355.

948 **Aulakh, K., and Durrett, T.P.** (2019). The Plastid Lipase PLIP1 Is Critical for Seed  
949 Viability in *diacylglycerol acyltransferase1* Mutant Seed. *Plant*  
950 *Physiol.* **180**, 1962-1974.

951 **Awai, K., Xu, C.C., Tamot, B., and Benning, C.** (2006). A phosphatidic acid-binding  
952 protein of the chloroplast inner envelope membrane involved in lipid trafficking.  
953 *Proc. Natl. Acad. Sci. U. S. A.* **103**, 10817-10822.

954 **Bastien, O., Botella, C., Chevalier, F., Block, M.A., Jouhet, J., Breton, C., Girard-**  
955 **Egrot, A., and Maréchal, E.** (2016). Chapter One - New Insights on Thylakoid  
956 Biogenesis in Plant Cells. In *International Review of Cell and Molecular Biology*,  
957 K.W. Jeon, ed (Academic Press), pp. 1-30.

958 **Bates, P.D.** (2016). Understanding the control of acyl flux through the lipid metabolic  
959 network of plant oil biosynthesis. *Biochimica et Biophysica Acta (BBA) -*  
960 *Molecular and Cell Biology of Lipids* **1861**, 1214-1225.

961 **Bates, P.D., Ohlrogge, J.B., and Pollard, M.** (2007). Incorporation of Newly  
962 Synthesized Fatty Acids into Cytosolic Glycerolipids in Pea Leaves Occurs via  
963 Acyl Editing. *J. Biol. Chem.* **282**, 31206-31216.

964 **Bates, P.D., Stymne, S., and Ohlrogge, J.** (2013). Biochemical pathways in seed oil  
965 synthesis. *Curr. Opin. Plant Biol.* **16**, 358-364.

966 **Bates, P.D., Durrett, T.P., Ohlrogge, J.B., and Pollard, M.** (2009). Analysis of Acyl  
967 Fluxes through Multiple Pathways of Triacylglycerol Synthesis in Developing  
968 Soybean Embryos. *Plant Physiol.* **150**, 55-72.

969 **Bates, P.D., Fatihi, A., Snapp, A.R., Carlsson, A.S., Browse, J., and Lu, C.** (2012).  
970 Acyl editing and headgroup exchange are the major mechanisms that direct  
971 polyunsaturated fatty acid flux into triacylglycerols. *Plant Physiol.* **160**, 1530-  
972 1539.

973 **Benning, C.** (2008). A role for lipid trafficking in chloroplast biogenesis. *Prog. Lipid Res.*  
974 **47**, 381-389.

975 **Benning, C.** (2009). Mechanisms of Lipid Transport Involved in Organelle Biogenesis in  
976 Plant Cells. *Annu. Rev. Cell Dev. Biol.* **25**, 71-91.

977 **Bessoule, J.J., Testet, E., and Cassagne, C.** (1995). Synthesis of phosphatidylcholine  
978 in the chloroplast envelope after import of lysophosphatidylcholine from  
979 endoplasmic-reticulum membranes. *Eur. J. Biochem.* **228**, 490-497.

980 **Block, M.A., and Jouhet, J.** (2015). Lipid trafficking at endoplasmic reticulum–  
981 chloroplast membrane contact sites. *Current Opinion in Cell Biology* **35**, 21-29.

982 **Botella, C., Jouhet, J., and Block, M.A.** (2017). Importance of phosphatidylcholine on  
983 the chloroplast surface. *Prog Lipid Res* **65**, 12-23.

984 **Botella, C., Sautron, E., Boudiere, L., Michaud, M., Dubots, E., Yamaryo-Botté, Y.,**  
985 **Albrieux, C., Marechal, E., Block, M.A., and Jouhet, J.** (2016). ALA10, a  
986 Phospholipid Flippase, Controls FAD2/FAD3 Desaturation of Phosphatidylcholine  
987 in the ER and Affects Chloroplast Lipid Composition in *Arabidopsis thaliana*.  
988 *Plant Physiol.* **170**, 1300-1314.

989 **Boudière, L., Michaud, M., Petroutsos, D., Rébeillé, F., Falconet, D., Bastien, O.,**  
990 **Roy, S., Finazzi, G., Rolland, N., Jouhet, J., Block, M.A., and Maréchal, E.**  
991 (2014). Glycerolipids in photosynthesis: Composition, synthesis and trafficking.  
992 *Biochimica et Biophysica Acta (BBA) - Bioenergetics* **1837**, 470-480.

993 **Browse, J., and Somerville, C.** (1991). Glycerolipid synthesis - biochemistry and  
994 regulation. *Annu. Rev. Plant Physiol. Plant Molec. Biol.* **42**, 467-506.

995 **Browse, J., Warwick, N., Somerville, C.R., and Slack, C.R.** (1986). Fluxes through  
996 the prokaryotic and eukaryotic pathways of lipid-synthesis in the 16:3 plant  
997 *Arabidopsis-thaliana*. *Biochem. J.* **235**, 25-31.

998 **Bulat, E., and Garrett, T.A.** (2011). Putative N-Acylphosphatidylethanolamine  
999 Synthase from *Arabidopsis thaliana* Is a Lysoglycerophospholipid  
1000 Acyltransferase. *J. Biol. Chem.* **286**, 33819-33831.

1001 **Dorne, A.J., Joyard, J., Block, M.A., and Douce, R.** (1985). Localization of  
1002 phosphatidylcholine in outer envelope membrane of spinach chloroplasts. *The*  
1003 *Journal of Cell Biology* **100**, 1690-1697.

1004 **Fan, J., Yan, C., and Xu, C.** (2013a). Phospholipid:diacylglycerol acyltransferase-  
1005 mediated triacylglycerol biosynthesis is crucial for protection against fatty acid-  
1006 induced cell death in growing tissues of *Arabidopsis*. *Plant J* **76**, 930-942.

1007 **Fan, J., Yan, C., Zhang, X., and Xu, C.** (2013b). Dual role for  
1008 phospholipid:diacylglycerol acyltransferase: enhancing fatty acid synthesis and  
1009 diverting fatty acids from membrane lipids to triacylglycerol in *Arabidopsis* leaves.  
1010 *Plant Cell* **25**, 3506-3518.

1011 **Fan, J., Zhai, Z., Yan, C., and Xu, C.** (2015). *Arabidopsis*  
1012 TRIGALACTOSYLDIACYLGLYCEROL5 interacts with TGD1, TGD2, and TGD4  
1013 to facilitate lipid transfer from the endoplasmic reticulum to plastids. *The Plant*  
1014 *Cell*, tpc. 15.00394.

1015 **Fan, J., Yan, C., Roston, R., Shanklin, J., and Xu, C.** (2014). *Arabidopsis* Lipins,  
1016 PDAT1 Acyltransferase, and SDP1 Triacylglycerol Lipase Synergistically Direct  
1017 Fatty Acids toward beta-Oxidation, Thereby Maintaining Membrane Lipid  
1018 Homeostasis. *Plant Cell* **26**, 4119-4134.

1019 **Gląb, B., Beganovic, M., Anaokar, S., Hao, M.-S., Rasmusson, A., Patton-Vogt, J.,**  
1020 **Banaś, A., Stymne, S., and Lager, I.** (2016). Cloning of glycerophosphocholine  
1021 acyltransferase (GPCAT) from fungi and plants; a novel enzyme in  
1022 phosphatidylcholine synthesis. *J. Biol. Chem.* **291**, 25066-25076.

1023 **Hara, A., and Radin, N.S.** (1978). Lipid extraction of tissues with a low-toxicity solvent.  
1024 *Anal. Biochem.* **90**, 420-426.

1025 **Hurlock, A.K., Roston, R.L., Wang, K., and Benning, C.** (2014). Lipid Trafficking in  
1026 Plant Cells. *Traffic* **15**, 915-932.

1027 **Hurlock, A.K., Wang, K., Takeuchi, T., Horn, P.J., and Benning, C.** (2018). In vivo  
1028 lipid 'tag and track' approach shows acyl editing of plastid lipids and chloroplast  
1029 import of phosphatidylglycerol precursors in *Arabidopsis thaliana*. *Plant J* **95**,  
1030 1129-1139.

1031 **Jarvis, P., Dörmann, P., Peto, C.A., Lutes, J., Benning, C., and Chory, J.** (2000).  
1032 Galactolipid deficiency and abnormal chloroplast development in the  
1033 <em>Arabidopsis MGD synthase 1</em> mutant. *Proceedings of the National*  
1034 *Academy of Sciences* **97**, 8175-8179.

1035 **Jasieniecka-Gazarkiewicz, K., Demski, K., Lager, I., Stymne, S., and Banas, A.**  
1036 (2016). Possible Role of Different Yeast and Plant Lysophospholipid:Acyl-CoA  
1037 Acyltransferases (LPLATs) in Acyl Remodelling of Phospholipids. *Lipids* **51**, 15-  
1038 23.

1039 **Jessen, D., Roth, C., Wiermer, M., and Fulda, M.** (2015). Two Activities of Long-Chain  
1040 Acyl-Coenzyme A Synthetase Are Involved in Lipid Trafficking between the  
1041 Endoplasmic Reticulum and the Plastid in *Arabidopsis*. *Plant Physiol.* **167**, 351-  
1042 366.

1043 **Kelly, A.A., and Dormann, P.** (2004). Green light for galactolipid trafficking. *Curr Opin*  
1044 *Plant Biol* **7**, 262-269.

1045 **Kim, H.U., Li, Y.B., and Huang, A.H.C.** (2005). Ubiquitous and endoplasmic reticulum-  
1046 located lysophosphatidyl acyltransferase, LPAT2, is essential for female but not  
1047 male gametophyte development in *Arabidopsis*. *Plant Cell* **17**, 1073-1089.

1048 **Koo, A.J.K., Ohlrogge, J.B., and Pollard, M.** (2004). On the export of fatty acids from  
1049 the chloroplast. *J. Biol. Chem.* **279**, 16101-16110.

1050 **Kubis, S.E., Lilley, K.S., and Jarvis, P.** (2008). Isolation and Preparation of  
1051 Chloroplasts from *Arabidopsis thaliana* Plants. In *2D PAGE: Sample Preparation*  
1052 and *Fractionation*, A. Posch, ed (Totowa, NJ: Humana Press), pp. 171-186.

1053 **Kunst, L., Browse, J., and Somerville, C.** (1988). Altered regulation of lipid  
1054 biosynthesis in a mutant of *Arabidopsis* deficient in chloroplast glycerol-3-  
1055 phosphate acyltransferase activity. *Proc. Natl. Acad. Sci. U. S. A.* **85**, 4143-4147.

1056 **LaBrant, E., Barnes, A.C., and Roston, R.L.** (2018). Lipid transport required to make  
1057 lipids of photosynthetic membranes. *Photosynthesis Research*.

1058 **Lager, I., Glab, B., Eriksson, L., Chen, G., Banas, A., and Stymne, S.** (2015). Novel  
1059 reactions in acyl editing of phosphatidylcholine by lysophosphatidylcholine  
1060 transacylase (LPCT) and acyl-CoA:glycerophosphocholine acyltransferase  
1061 (GPCAT) activities in microsomal preparations of plant tissues. *Planta* **241**, 347-  
1062 358.

1063 **Lager, I., Yilmaz, J.L., Zhou, X.-R., Jasieniecka, K., Kazachkov, M., Wang, P., Zou,**  
1064 **J., Weselake, R., Smith, M.A., Bayon, S., Dyer, J.M., Shockley, J.M., Heinz,**  
1065 **E., Green, A., Banas, A., and Stymne, S.** (2013). Plant Acyl-

1066 CoA:Lysophosphatidylcholine Acyltransferases (LPCATs) Have Different  
1067 Specificities in Their Forward and Reverse Reactions. *J. Biol. Chem.* **288**, 36902-  
1068 36914.

1069 **Lands, W.E.M.** (1965). Lipid metabolism. *Annu. Rev. Biochem.* **34**, 313-&.

1070 **Larsson, K.E., Kjellberg, J.M., Tjellstrom, H., and Sandelius, A.S.** (2007). LysoPC  
1071 acyltransferase/PC transacylase activities in plant plasma membrane and plasma  
1072 membrane-associated endoplasmic reticulum. *BMC Plant Biol.* **7**, 12.

1073 **Li-Beisson, Y., Neunzig, J., Lee, Y., and Philipp, K.** (2017). Plant membrane-  
1074 protein mediated intracellular traffic of fatty acids and acyl lipids. *Curr. Opin.*  
1075 *Plant Biol.* **40**, 138-146.

1076 **Li-Beisson, Y., Shorrosh, B., Beisson, F., Andersson, M.X., Arondel, V., Bates,**  
1077 **P.D., Baud, S., Bird, D., Debono, A., Durrett, T.P., Franke, R.B., Graham, I.A.,**  
1078 **Katayama, K., Kelly, A.A., Larson, T., Markham, J.E., Miquel, M., Molina, I.,**  
1079 **Nishida, I., Rowland, O., Samuels, L., Schmid, K.M., Wada, H., Welti, R., Xu,**  
1080 **C., Zallot, R., and Ohlrogge, J.** (2013). Acyl-lipid metabolism. *The Arabidopsis*  
1081 book / American Society of Plant Biologists **11**, e0161.

1082 **Li, N., Gügel, I.L., Giavalisco, P., Zeisler, V., Schreiber, L., Soll, J., and Philipp,**  
1083 **K.** (2015). FAX1, a Novel Membrane Protein Mediating Plastid Fatty Acid Export.  
1084 *PLoS Biol* **13**, e1002053.

1085 **Lu, B., and Benning, C.** (2009). A 25-Amino Acid Sequence of the Arabidopsis TGD2  
1086 Protein Is Sufficient for Specific Binding of Phosphatidic Acid. *J. Biol. Chem.* **284**,  
1087 17420-17427.

1088 **Lu, B., Xu, C., Awai, K., Jones, A.D., and Benning, C.** (2007). A small ATPase protein  
1089 of Arabidopsis, TGD3, involved in chloroplast lipid import. *J. Biol. Chem.* **282**,  
1090 35945-35953.

1091 **Maatta, S., Scheu, B., Roth, M.R., Tamura, P., Li, M., Williams, T.D., Wang, X., and**  
1092 **Welti, R.** (2012). Levels of Arabidopsis thaliana leaf phosphatidic acids,  
1093 phosphatidylserines, and most trienoate-containing polar lipid molecular species  
1094 increase during the dark period of the diurnal cycle. *Frontiers in Plant Science* **3**,  
1095 49.

1096 **Maréchal, E., and Bastien, O.** (2014). Modeling of regulatory loops controlling  
1097 galactolipid biosynthesis in the inner envelope membrane of chloroplasts. *Journal*  
1098 of Theoretical Biology **361**, 1-13.

1099 **Meï, C., Michaud, M., Cussac, M., Albrieux, C., Gros, V., Maréchal, E., Block, M.A.,**  
1100 **Jouhet, J., and Rébeillé, F.** (2015). Levels of polyunsaturated fatty acids  
1101 correlate with growth rate in plant cell cultures. *Scientific reports* **5**, 15207.

1102 **Mongrand, S., Bessoule, J.J., and Cassagne, C.** (1997). A re-examination *in vivo* of  
1103 the phosphatidylcholine-galactolipid metabolic relationship during plant lipid  
1104 biosynthesis. *Biochem. J.* **327**, 853-858.

1105 **Mongrand, S., Cassagne, C., and Bessoule, J.J.** (2000). Import of lyso-  
1106 phosphatidylcholine into chloroplasts likely at the origin of eukaryotic plastidial  
1107 lipids. *Plant Physiol.* **122**, 845-852.

1108 **Mongrand, S., Bessoule, J.J., Cabantous, F., and Cassagne, C.** (1998). The C-16 :  
1109 3/C-18 : 3 fatty acid balance in photosynthetic tissues from 468 plant species.  
1110 *Phytochemistry* **49**, 1049-1064.

1111 **Moreau, P., Bessoule, J.J., Mongrand, S., Testet, E., Vincent, P., and Cassagne, C.**  
1112 (1998). Lipid trafficking in plant cells. *Prog. Lipid Res.* **37**, 371-391.

1113 **Mueller-Schuessele, S.J., and Michaud, M.** (2018). Plastid Transient and Stable  
1114 Interactions with Other Cell Compartments. In *Plastids: Methods and Protocols*,  
1115 E. Maréchal, ed (New York, NY: Springer US), pp. 87-109.

1116 **Nakamura, Y., Koizumi, R., Shui, G., Shimojima, M., Wenk, M.R., Ito, T., and Ohta,**  
1117 H. (2009). Arabidopsis lipins mediate eukaryotic pathway of lipid metabolism and  
1118 cope critically with phosphate starvation. *Proceedings of the National Academy of*  
1119 *Sciences*, -.

1120 **Nishida, I., Tasaka, Y., Shiraishi, H., and Murata, N.** (1993). The gene and the RNA  
1121 for the precursor to the plastid-located glycerol-3-phosphate acyltransferase of  
1122 *Arabidopsis thaliana*. *Plant Mol Biol* **21**, 267-277.

1123 **Ohlrogge, J., and Browse, J.** (1995). Lipid Biosynthesis. *Plant Cell* **7**, 957-970.

1124 **Okuley, J., Lightner, J., Feldmann, K., Yadav, N., Lark, E., and Browse, J.** (1994).  
1125 *Arabidopsis FAD2* gene encodes the enzyme that is essential for  
1126 polyunsaturated lipid-synthesis. *Plant Cell* **6**, 147-158.

1127 **Roughan, P.G., and Slack, C.R.** (1982). Cellular-organization of glycerolipid  
1128 metabolism. *Annu. Rev. Plant Physiol. Plant Molec. Biol.* **33**, 97-132.

1129 **Schnurr, J.A., Shockley, J.M., de Boer, G.J., and Browse, J.A.** (2002). Fatty acid  
1130 export from the chloroplast. Molecular characterization of a major plastidial acyl-  
1131 coenzyme A synthetase from *Arabidopsis*. *Plant Physiol.* **129**, 1700-1709.

1132 **Shimojima, M., Ohta, H., and Nakamura, Y.** (2009). Biosynthesis and function of  
1133 chloroplast lipids. In *Lipids in Photosynthesis* (Springer), pp. 35-55.

1134 **Shockley, J., Regmi, A., Cotton, K., Adhikari, N., Browse, J., and Bates, P.D.** (2016).  
1135 Identification of *Arabidopsis* GPAT9 (At5g60620) as an Essential Gene Involved  
1136 in Triacylglycerol Biosynthesis. *Plant Physiol.* **170**, 163-179.

1137 **Singer, S.D., Chen, G., Mietkiewska, E., Tomasi, P., Jayawardhane, K., Dyer, J.M.,**  
1138 **and Weselake, R.J.** (2016). *Arabidopsis* GPAT9 contributes to synthesis of  
1139 intracellular glycerolipids but not surface lipids. *J Exp Bot* **67**, 4627-4638.

1140 **Slack, C.R., Roughan, P.G., and Balasingham, N.** (1977). Labeling studies *in vivo* on  
1141 metabolism of acyl and glycerol moieties of glycerolipids in developing maize  
1142 leaf. *Biochem. J.* **162**, 289-296.

1143 **Stahl, U., Stalberg, K., Stymne, S., and Ronne, H.** (2008). A family of eukaryotic  
1144 lysophospholipid acyltransferases with broad specificity. *FEBS Lett* **582**, 305-  
1145 309.

1146 **Stalberg, K., Stahl, U., Stymne, S., and Ohlrogge, J.** (2009). Characterization of two  
1147 *Arabidopsis thaliana* acyltransferases with preference for  
1148 lysophosphatidylethanolamine. *BMC Plant Biol.* **9**.

1149 **Tjellström, H., Strawsine, M., and Ohlrogge, J.B.** (2015). Tracking synthesis and  
1150 turnover of triacylglycerol in leaves. *J. Exp. Bot.* **66**, 1453-1461.

1151 **Tjellström, H., Yang, Z., Allen, D.K., and Ohlrogge, J.B.** (2012). Rapid Kinetic  
1152 Labeling of *Arabidopsis* Cell Suspension Cultures: Implications for Models of  
1153 Lipid Export from Plastids. *Plant Physiol.* **158**, 601-611.

1154 **Wang, K., Froehlich, J.E., Zienkiewicz, A., Hersh, H.L., and Benning, C.** (2017). A  
1155 Plastid Phosphatidylglycerol Lipase Contributes to the Export of Acyl Groups  
1156 from Plastids for Seed Oil Biosynthesis. *The Plant Cell* **29**, 1678-1696.

1157 **Wang, L., Kazachkov, M., Shen, W., Bai, M., Wu, H., and Zou, J.** (2014). Deciphering  
1158 the roles of Arabidopsis LPCAT and PAH in phosphatidylcholine homeostasis  
1159 and pathway coordination for chloroplast lipid synthesis. *Plant J* **80**, 965-976.

1160 **Wang, L., Shen, W., Kazachkov, M., Chen, G., Chen, Q., Carlsson, A.S., Stymne, S., Weselake, R.J., and Zou, J.** (2012a). Metabolic Interactions between the  
1161 Lands Cycle and the Kennedy Pathway of Glycerolipid Synthesis in Arabidopsis  
1162 Developing Seeds. *The Plant Cell Online* **24**, 4652-4669.

1164 **Wang, Z., Xu, C., and Benning, C.** (2012b). TGD4 involved in endoplasmic reticulum-  
1165 to-chloroplast lipid trafficking is a phosphatidic acid binding protein. *The Plant  
1166 Journal* **70**, 614-623.

1167 **Wang, Z., Anderson, N.S., and Benning, C.** (2013). The Phosphatidic Acid Binding  
1168 Site of the Arabidopsis Trigalactosyldiacylglycerol 4 (TGD4) Protein Required for  
1169 Lipid Import into Chloroplasts. *J. Biol. Chem.* **288**, 4763-4771.

1170 **Williams, J.P., Imperial, V., Khan, M.U., and Hodson, J.N.** (2000). The role of  
1171 phosphatidylcholine in fatty acid exchange and desaturation in *Brassica napus* L.  
1172 leaves. *Biochem. J.* **349**, 127-133.

1173 **Xu, C., and Shanklin, J.** (2016). Triacylglycerol Metabolism, Function, and  
1174 Accumulation in Plant Vegetative Tissues. *Annu. Rev. Plant Biol.* **67**, 179-206.

1175 **Xu, C., Fan, J., Froehlich, J.E., Awai, K., and Benning, C.** (2005). Mutation of the  
1176 TGD1 Chloroplast Envelope Protein Affects Phosphatidate Metabolism in  
1177 Arabidopsis. *Plant Cell* **17**, 3094-3110.

1178 **Xu, C., Yu, B., Cornish, A.J., Froehlich, J.E., and Benning, C.** (2006).  
1179 Phosphatidylglycerol biosynthesis in chloroplasts of Arabidopsis mutants  
1180 deficient in acyl-ACP glycerol-3- phosphate acyltransferase. *The Plant Journal*  
1181 **47**, 296-309.

1182 **Xu, C.C., Fan, J.L., Riekhof, W., Froehlich, J.E., and Benning, C.** (2003). A  
1183 permease-like protein involved in ER to thylakoid lipid transfer in Arabidopsis.  
1184 *Embo J.* **22**, 2370-2379.

1185 **Xu, J., Carlsson, A., Francis, T., Zhang, M., Hoffmann, T., Giblin, M., and Taylor, D.**  
1186 (2012). Triacylglycerol synthesis by PDAT1 in the absence of DGAT1 activity is  
1187 dependent on re-acylation of LPC by LPCAT2. *BMC Plant Biol.* **12**, 4.

1188 **Yang, W., Wang, G., Li, J., Bates, P.D., Wang, X., and Allen, D.K. (2017).**  
1189 Phospholipase Dzeta Enhances Diacylglycerol Flux into Triacylglycerol. *Plant*  
1190 *Physiol* **174**, 110-123.  
1191 **Yin, C., Andersson, M.X., Zhang, H., and Aronsson, H. (2015).** Phosphatidylcholine  
1192 is transferred from chemically-defined liposomes to chloroplasts through proteins  
1193 of the chloroplast outer envelope membrane. *FEBS Lett* **589**, 177-181.  
1194 **Yu, B., Wakao, S., Fan, J., and Benning, C. (2004).** Loss of Plastidic Lysophosphatidic  
1195 Acid Acyltransferase Causes Embryo-Lethality in *Arabidopsis*. *Plant Cell Physiol.*  
1196 **45**, 503-510.  
1197 **Zhao, L., Katavic, V., Li, F., Haughn, G.W., and Kunst, L. (2010).** Insertional mutant  
1198 analysis reveals that long-chain acyl-CoA synthetase 1 (LACS1), but not LACS8,  
1199 functionally overlaps with LACS9 in *Arabidopsis* seed oil biosynthesis. *Plant J* **64**,  
1200 1048-1058.

1201

1202 **Figure legends**

1203

1204 **Figure 1. Model of wild-type *Arabidopsis* acyl trafficking within leaf glycerolipid**  
1205 **synthesis**

1206 The model focuses on the trafficking of acyl groups between the chloroplast and the ER  
1207 for MGDG synthesis. The model is centered around the ER “PC pool”, which is involved  
1208 in *de novo* PC synthesis, desaturation, acyl editing, and turnover to produce the  
1209 substrate for MGDG production. Chloroplast OEM PC produced from transfer of LPC or  
1210 PC may also be a substrate for MGDG synthesis. Key enzymes/transporters are in  
1211 yellow, uncertain reactions are in blue and have dashed lines. Abbreviations are as in  
1212 text.

1213

1214 **Figure 2. Membrane lipid composition of leaves across development from wild-**  
1215 **type and mutant lines.** The relative abundance of leaf membrane lipids was  
1216 determined at three developmental stages: two weeks (A), three weeks (B), and four  
1217 weeks (C) after germination. The data represent the average and standard error of 2-4  
1218 biological replicates. Significant (P-value < 0.05, Two-way ANOVA with multiple

1219 comparisons) differences within individual lipid abundances between *act1* and *act1*  
1220 *lpcat1 lpcat2* are indicated by asterisks above the bars.

1221

1222 **Figure 3. Fatty acid composition of PC and PE across leaf development from wild-**  
1223 **type and mutant lines.** The fatty acid composition of PC (A-C) and PE (D-F) were  
1224 determined at three developmental stages: two weeks (A, D), three weeks (B, E), and  
1225 four weeks (C, F) after germination. The data represent the average and standard error  
1226 of 2-4 biological replicates. Significant (p-value < 0.05, Two-way ANOVA with multiple  
1227 comparisons) differences within individual lipid abundances between *act1* and *act1*  
1228 *lpcat1 lpcat2* are indicated by asterisks above the bars.

1229

1230 **Figure 4. LPCAT activity in isolated chloroplasts.** Isolated chloroplasts from Col-0,  
1231 *act1*, *lpcat1 lpcat2*, and *act1 lpcat1 lpcat2* were incubated with 1 mM soy LPC, and 13.6  
1232  $\mu$ M [ $^{14}$ C]oleoyl-CoA for 30 min at 30 °C and radioactivity incorporated into PC  
1233 measured. The data represent the average and SEM of three independent assays from  
1234 chloroplasts isolated from each line. Significant (p-value < 0.05, students t-test)  
1235 differences from the Col-0 control are indicated by asterisks above the bars.

1236

1237 **Figure 5. Initial incorporation of [ $^{14}$ C]acetate-labeled nascent fatty acids into leaf**  
1238 **lipids.** Continuous [ $^{14}$ C]acetate labeling of 3-week-old leaves over a 1 hour time course.  
1239 (A) Total  $^{14}$ C accumulation in organic extractable lipids, and linear regression.  
1240 Significant differences (students t-test, p-value <0.05) in lipid labeling between lines at  
1241 each time point are indicated by asterisks above the data points. (B-C) Incorporation of  
1242 [ $^{14}$ C]acetate into major labeled membrane lipids and DAG in the *act1* and *act1 lpcat1*  
1243 *lpcat2* lines respectively.

1244

1245 **Figure 6. Relative accumulation of [ $^{14}$ C]acetate-labeled nascent fatty acids into**  
1246 **leaf lipids.** The relative labeling of individual lipids to the total labeled lipids in each line  
1247 compared between lines. (A) PC. (B) DAG and PA. (C) PE, PG, and PI/PS. (D) MGDG.  
1248 All data points are average and SEM from three sets of independently-labeled plants.  
1249 Significant differences (students t-test, p-value <0.05) in lipid labeling between lines at

1250 each time point are indicated by asterisks above the data points. An  $\alpha$  above the data  
1251 indicates a p-value  $<0.07$ .

1252

1253 **Figure 7. Stereochemical analysis of [<sup>14</sup>C]acetate-labeled nascent fatty acids**  
1254 **incorporation into DAG and PC.** Continuous [<sup>14</sup>C]acetate-labeled DAG and PC from  
1255 Figures 5 and 6 were collected and subjected to lipase-based regiochemical analysis of  
1256 <sup>14</sup>C fatty acid locations in the *sn*-1 or *sn*-2 position of the glycerol backbone. (A) *act1*  
1257 DAG. (B) *act1 lpcat1 lpcat2* DAG. (C) *act1* PC. (D) *act1 lpcat1 lpcat2* PC. All data points  
1258 are average and SEM from three sets of independently-labeled plants.

1259

1260 **Figure 8. Pulse-chase [<sup>14</sup>C]acetate tracking of leaf lipid precursor–product**  
1261 **relationships.** A 15 min [<sup>14</sup>C]acetate pulse of 3-week-old whole rosettes was followed  
1262 by a chase up to 51 hours. (A-B) Relative labeling of lipids within *act1* (A), or *act1*  
1263 *lpcat1 lpcat2* (B). (C-F) Relative labeling of major labeled individual lipids to the total  
1264 labeled lipids in each line compared between lines. (C) PC and DAG. (D) MGDG. (E)  
1265 PE and PA. (F) TAG. All data points are average and SEM from three sets of  
1266 independently-labeled plants, except for PA which had 1–3 replicates. In (C-F),  
1267 significant differences (students t-test, p-value  $<0.05$ ) in lipid labeling between lines at  
1268 each time point are indicated by asterisks above the data points.

1269

1270 **Figure 9. Radiolabeled fatty acid composition of DAG, PC, and MGDG over the**  
1271 **[<sup>14</sup>C]acetate pulse-chase time course.** The radiolabeled fatty acids in different lipids  
1272 from Fig. 8 are represented as total saturated fatty acids (e.g. 16:0, 18:0), monoenoic  
1273 fatty acids (e.g. 18:1), dienoic (e.g. 18:2), and trienoic (e.g. 18:3). The proportion of  
1274 each fatty acid within each lipid is compared between plant lines with *act1* as solid lines,  
1275 and *act1 lpcat1 lpcat2* as dashed lines. (A-B) DAG. (C-D) PC. (E-F) MGDG. All data  
1276 points are average and SEM from three sets of independently-labeled plants from Fig.  
1277 8. Significant differences (students t-test, p-value  $<0.05$ ) in lipid labeling between lines  
1278 at each time point are indicated by asterisks above the data points.

1279

1280 **Figure 10. Stereochemical analysis of [<sup>14</sup>C]acetate-labeled fatty acids within DAG,**  
1281 **PC, and MGDG over the pulse-chase time course.** The *sn*-1 position is solid lines;  
1282 the *sn*-2 position is dashed lines. The *act1* samples are blue lines; the *act1 lpcat1 lpcat2*  
1283 samples are red lines. (A) DAG. (B) PC. (C) MGDG. All data points are average and  
1284 SEM from three sets of independently-labeled plants from Fig. 8. Significant differences  
1285 (students t-test, p-value <0.05) in lipid labeling between *act1* and *act1 lpcat1 lpcat2*  
1286 stereochemical positions at each time point are indicated by asterisks next to the *act1*  
1287 blue lines in (B), and next to the *act1 lpcat1 lpcat2* red lines in (C).

1288

1289 **Figure 11: Models of [<sup>14</sup>C]acetate pulse-chase labeling of MGDG synthesis in *act1***  
1290 **and *act1 lpcat1 lpcat2* leaves.**

1291 The models indicate the relative rate of labeled fatty acid flux through the eukaryotic  
1292 pathway of MGDG synthesis within the pulse-chase experiment. Red solid lines  
1293 represent initial reactions, blue large dashed lines represent the next set of reactions  
1294 labeled over time, and the green small dashed lines represent the slowest set of  
1295 reactions labeled over time within each model. Likewise, for the DAG, PC, and MGDG  
1296 pools, the major labeled stereochemical position at various time points is indicated by  
1297 the position noted with an asterisk and color coding the same as the lines. No specific  
1298 time points are intended, and each model color coding is independent from the others,  
1299 representing only relative labeling within each model. Abbreviations are as in the text. A,  
1300 *act1*. B, *act1 lpcat1 lpcat2* with no PC acyl chain removal from residual acyl-editing  
1301 mechanisms. C, *act1 lpcat1 lpcat2* with compensating acyl-editing reactions that lead to  
1302 acyl chain removal from PC and incorporation into the acyl-CoA pool, and the switching  
1303 of PC labeled stereochemistry from *sn*-1 to *sn*-2.

1304

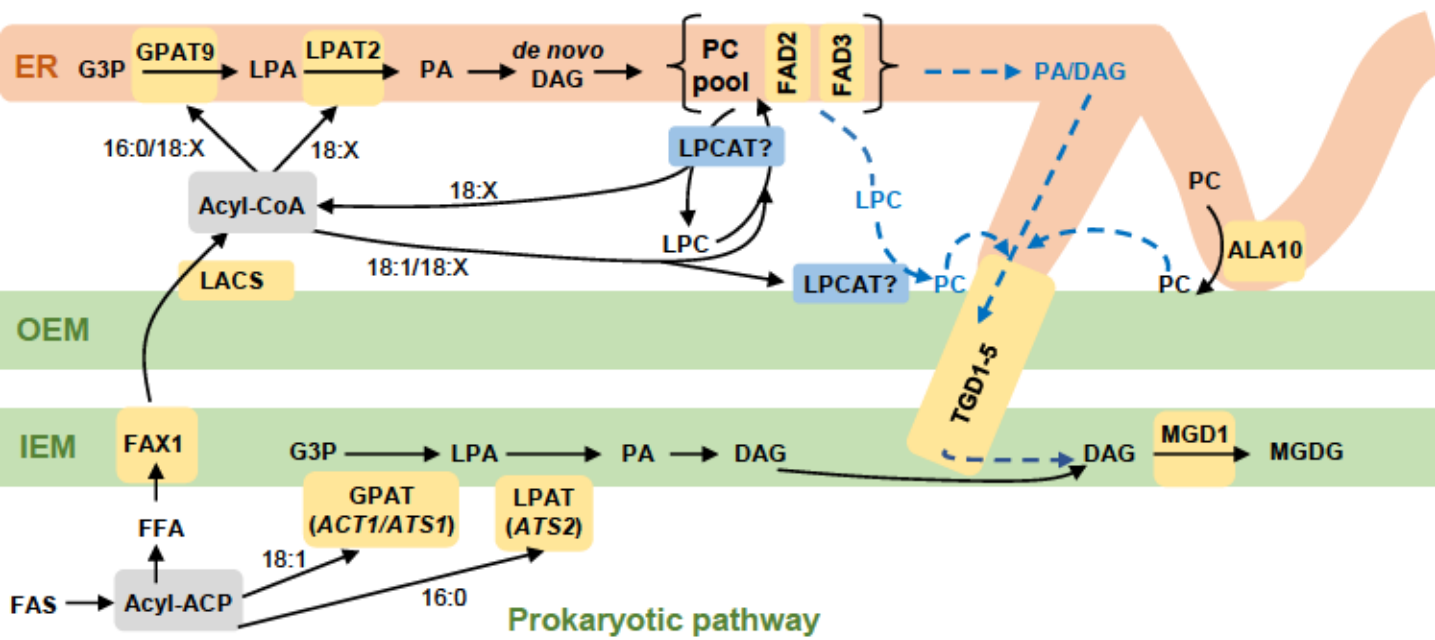
1305 **Figure 12. Updated model of wild-type *Arabidopsis* acyl trafficking within leaf**  
1306 **glycerolipid assembly clarifying the role of LPCAT1 and LPCAT2.**

1307 The model focuses on the trafficking of acyl groups between the chloroplast and the ER  
1308 for MGDG synthesis. Here the model separates PC involved in acyl editing “PC(1)” from  
1309 PC synthesized *de novo* “PC(2)” and PC that provides the substrate for MGDG  
1310 synthesis “PC(3)”. The model also allows that PC acyl editing may take place in the ER

1311 or at the chloroplast surface, which could be a way to move acyl groups into the ER by  
1312 PC movement through membrane contact sites. The PC(3) pool is derived from *de novo*  
1313 synthesized PC(2) which may have been further desaturated by FAD2 and FAD3. The  
1314 substrate for MGDG synthesis may come from turnover of the PC(3) pool in the ER, or  
1315 turnover of the PC(3) at the chloroplast surface. Key enzymes/transporters are in  
1316 yellow, uncertain reactions are in blue and have dashed lines. Abbreviations are as in  
1317 text, rLPCAT is the reverse LPCAT reaction

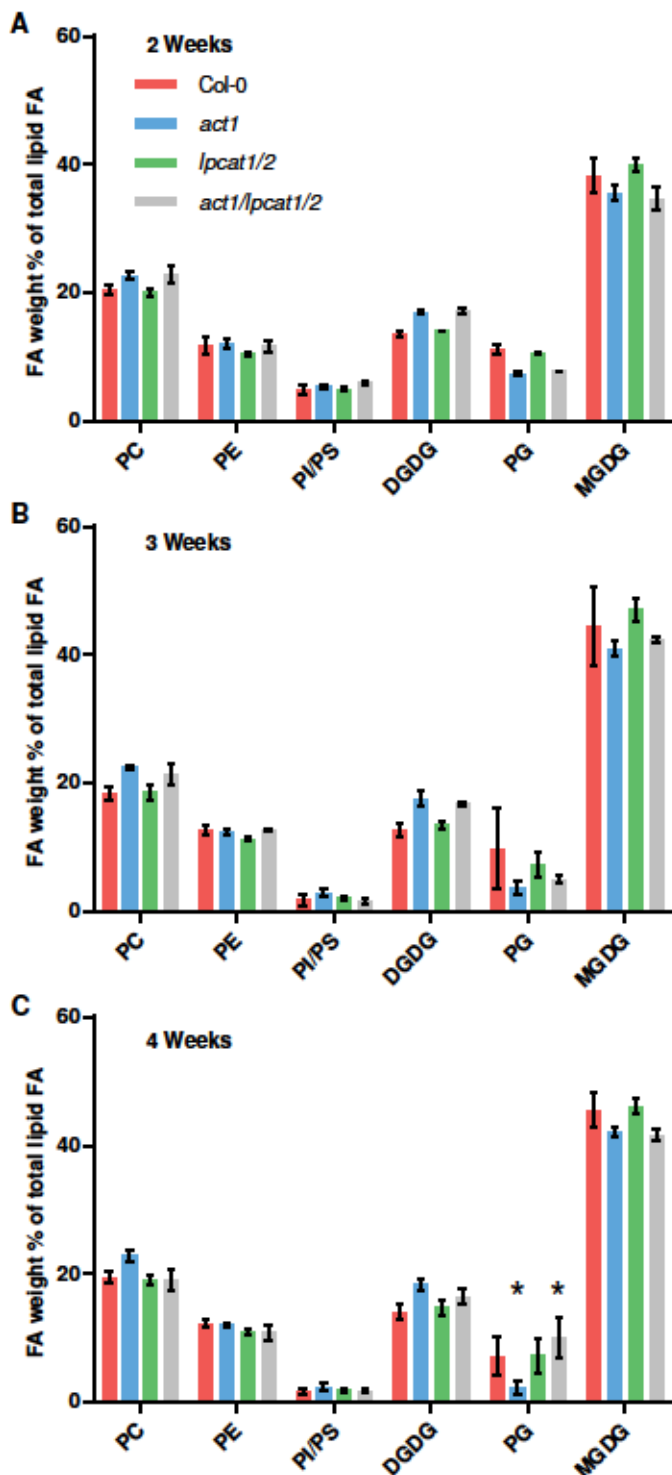
1318

## Eukaryotic pathway

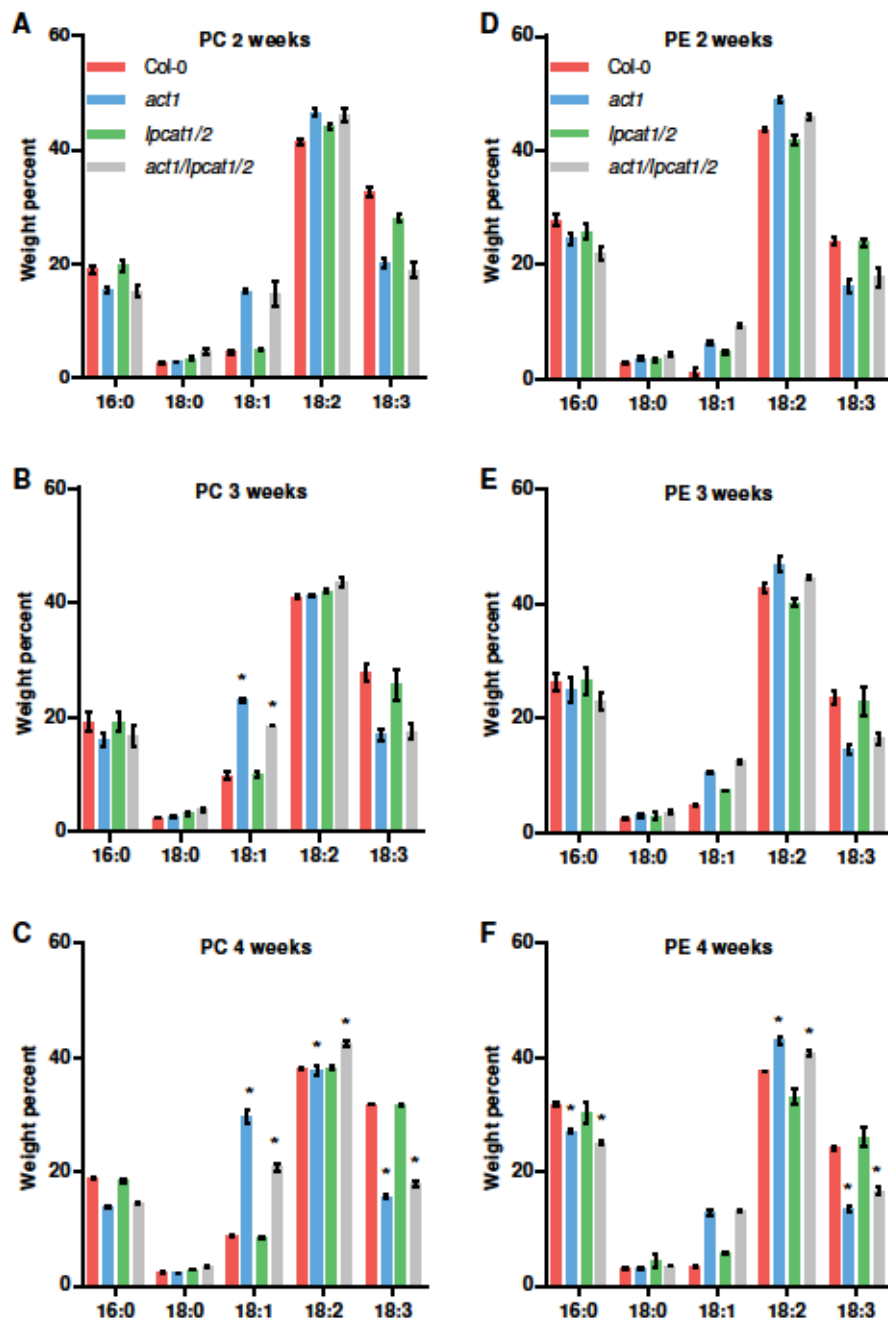


**Figure 1. Model of wild-type *Arabidopsis* acyl trafficking within leaf glycerolipid synthesis**

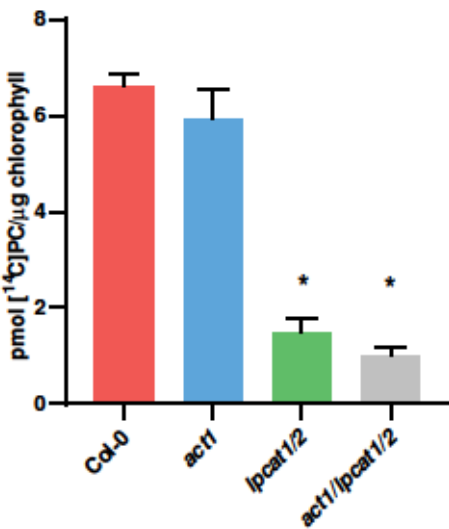
The model focuses on the trafficking of acyl groups between the chloroplast and the ER for MGDG synthesis. The model is centered around the ER “PC pool” which is involved in *de novo* PC synthesis, desaturation, acyl editing, and turnover to produce the substrate for MGDG production. Chloroplast OEM PC produced from transfer of LPC or PC may also be a substrate for MGDG synthesis. Key enzymes/transporters are in yellow, uncertain reactions are in blue and have dashed lines. Abbreviations are as in text.



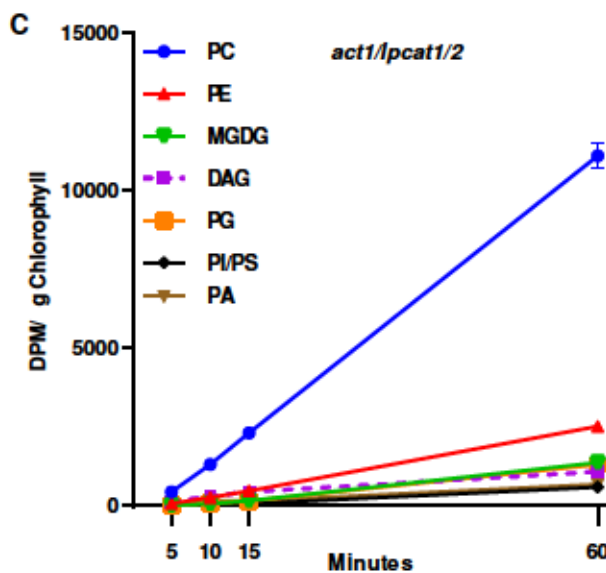
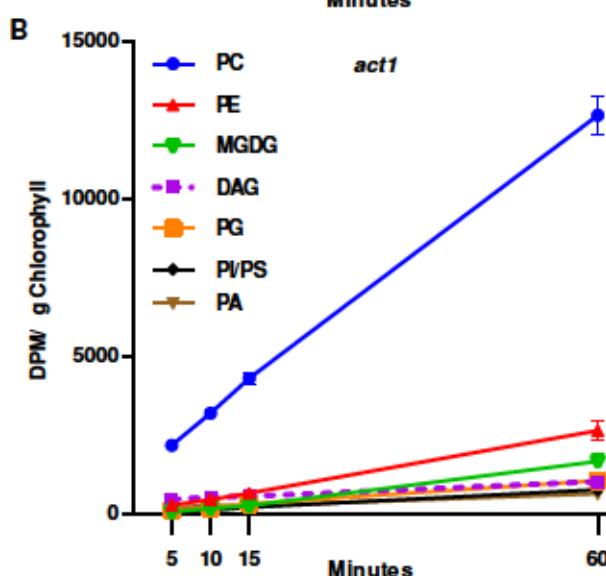
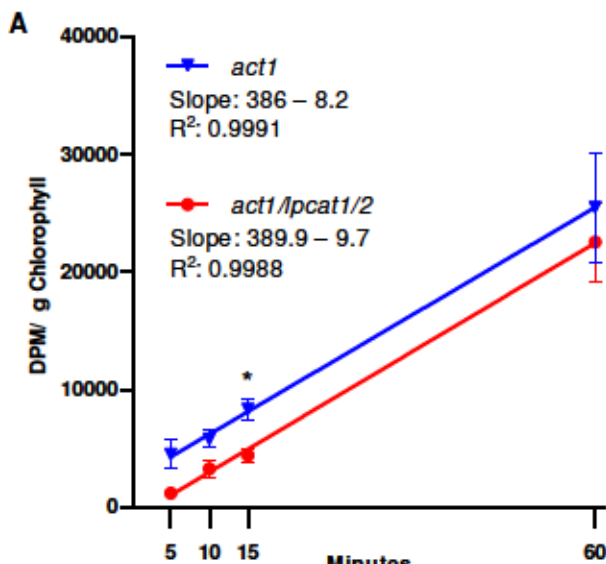
**Figure 2. Membrane lipid composition of leaves across development from wild-type and mutant lines.** The relative abundance of leaf membrane lipids was determined at three developmental stages: two weeks (A), three weeks (B), and four weeks (C) after germination. The data represents the average and standard error of 2-4 biological replicates. Significant (P-value < 0.05, Two-way ANOVA with multiple comparisons) differences within individual lipid abundances between *act1* and *act1/lpcat1/2* are indicated by asterisks above the bars.



**Figure 3. Fatty acid composition of PC and PE across leaf development from wild-type and mutant lines.** The fatty acid composition of PC (A-C) and PE (D-F) were determined at three developmental stages: two weeks (A, D), three weeks (B, E), and four weeks (C, F) after germination. The data represents the average and standard error of 2-4 biological replicates. Significant ( $p$ -value  $< 0.05$ , Two-way ANOVA with multiple comparisons) differences within individual lipid abundances between *act1* and *act1/lpcat1/2* are indicated by asterisks above the bars.



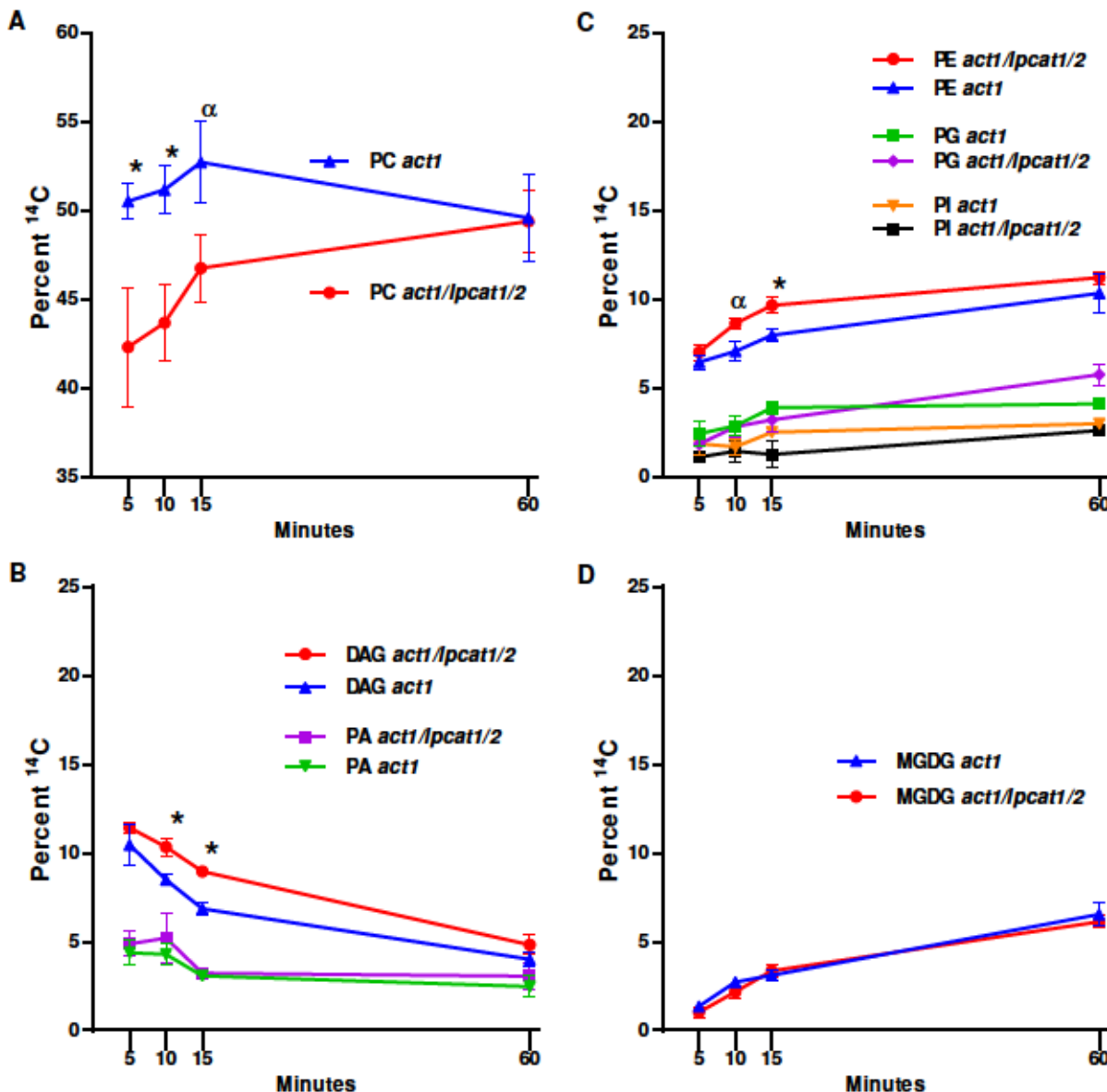
**Figure 4. LPCAT activity in isolated chloroplasts.** Isolated chloroplasts from Col-0, *act1*, *lpcat1/2*, and *act1/lpcat1/2* were incubated with 1mM soy LPC, and 13.6 M  $[^{14}\text{C}]$ oleoyl-CoA for 30 min at 30 °C and radioactivity incorporated into PC measured. The data represents the average and SEM of three independent assays from chloroplasts isolated from each line. Significant (p-value < 0.05, students t-test) differences from the Col-0 control are indicated by asterisks above the bars.



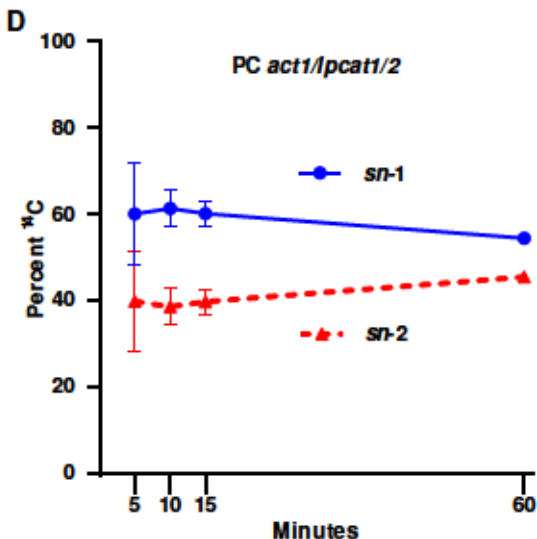
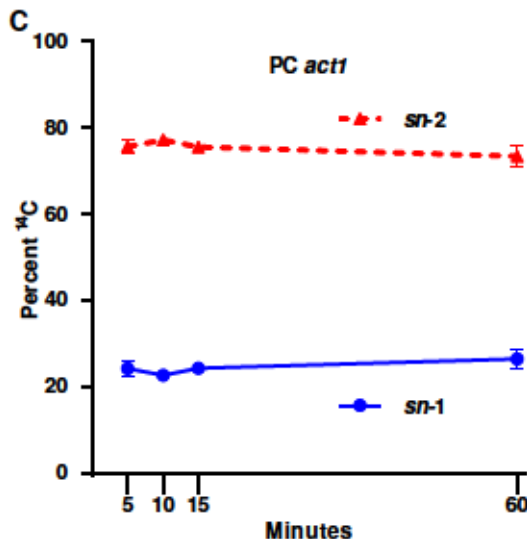
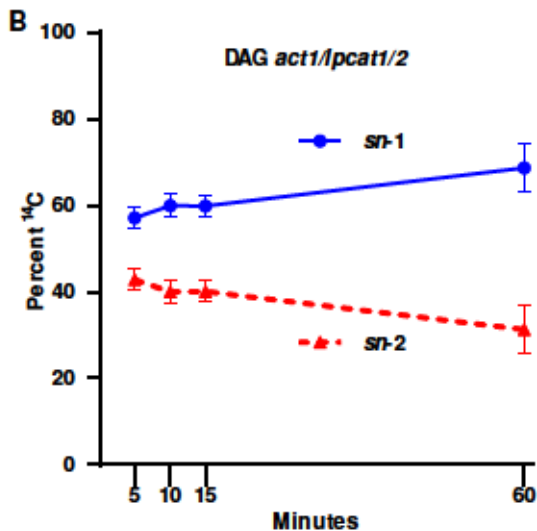
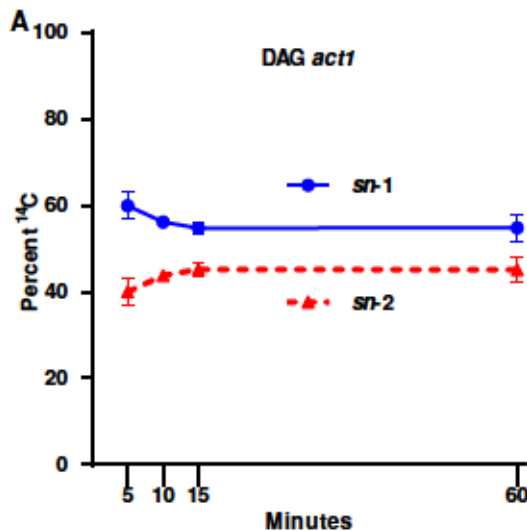
**Figure 5. Initial incorporation of [<sup>14</sup>C]acetate labeled nascent fatty acids into leaf lipids.**

Continuous [<sup>14</sup>C]acetate labeling of 3 week old leaves over a 1 hour time course. (A) total <sup>14</sup>C accumulation in organic extractable lipids, and linear regression. Significant differences (students t-test,  $p$ -value <0.05) in lipid labeling between lines at each time point is indicated by an asterisk above the data point. (B-C),

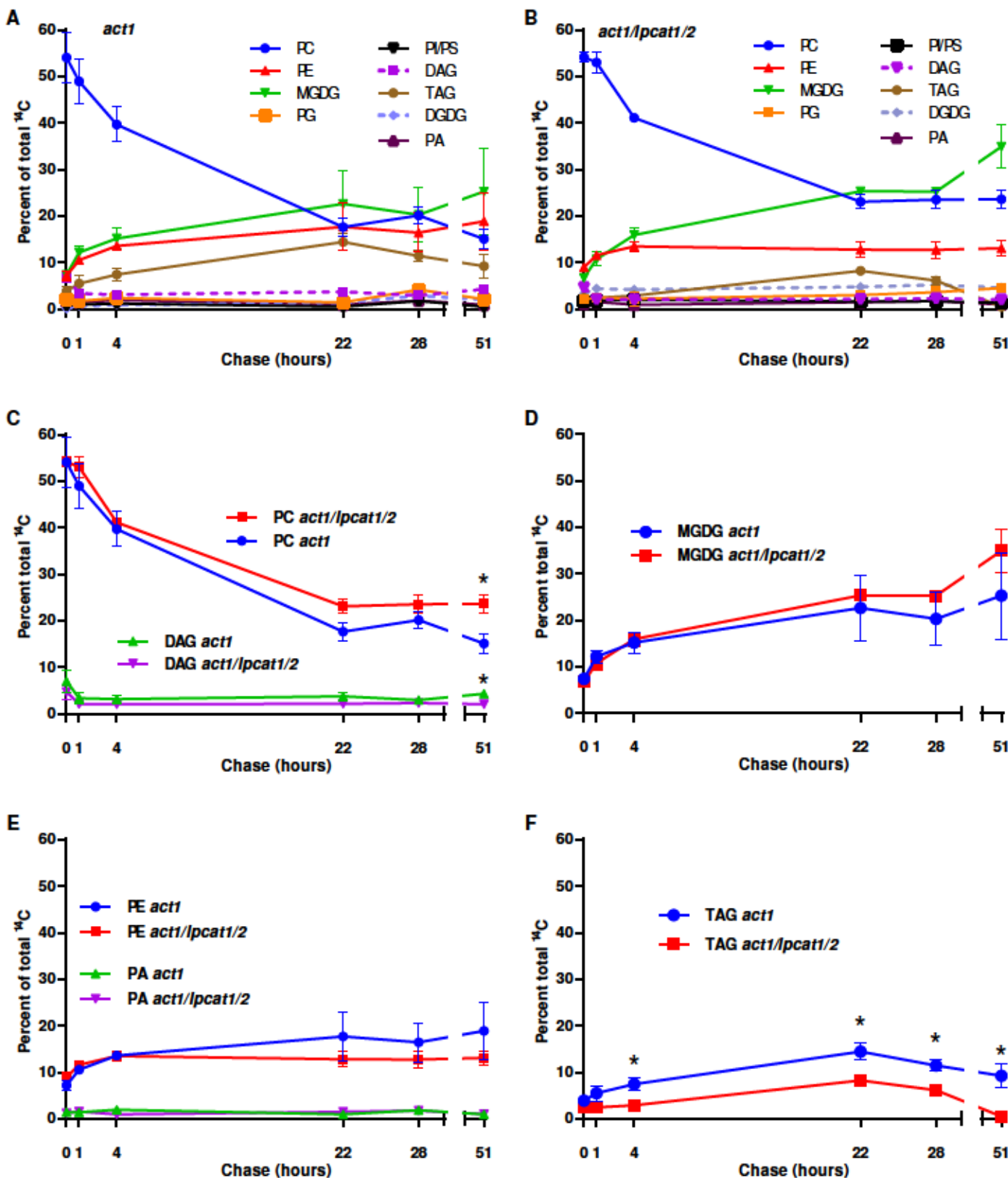
incorporation of [<sup>14</sup>C]acetate into major labeled membrane lipids and DAG in the *act1* and *act1/lpcat1/2* lines respectively.



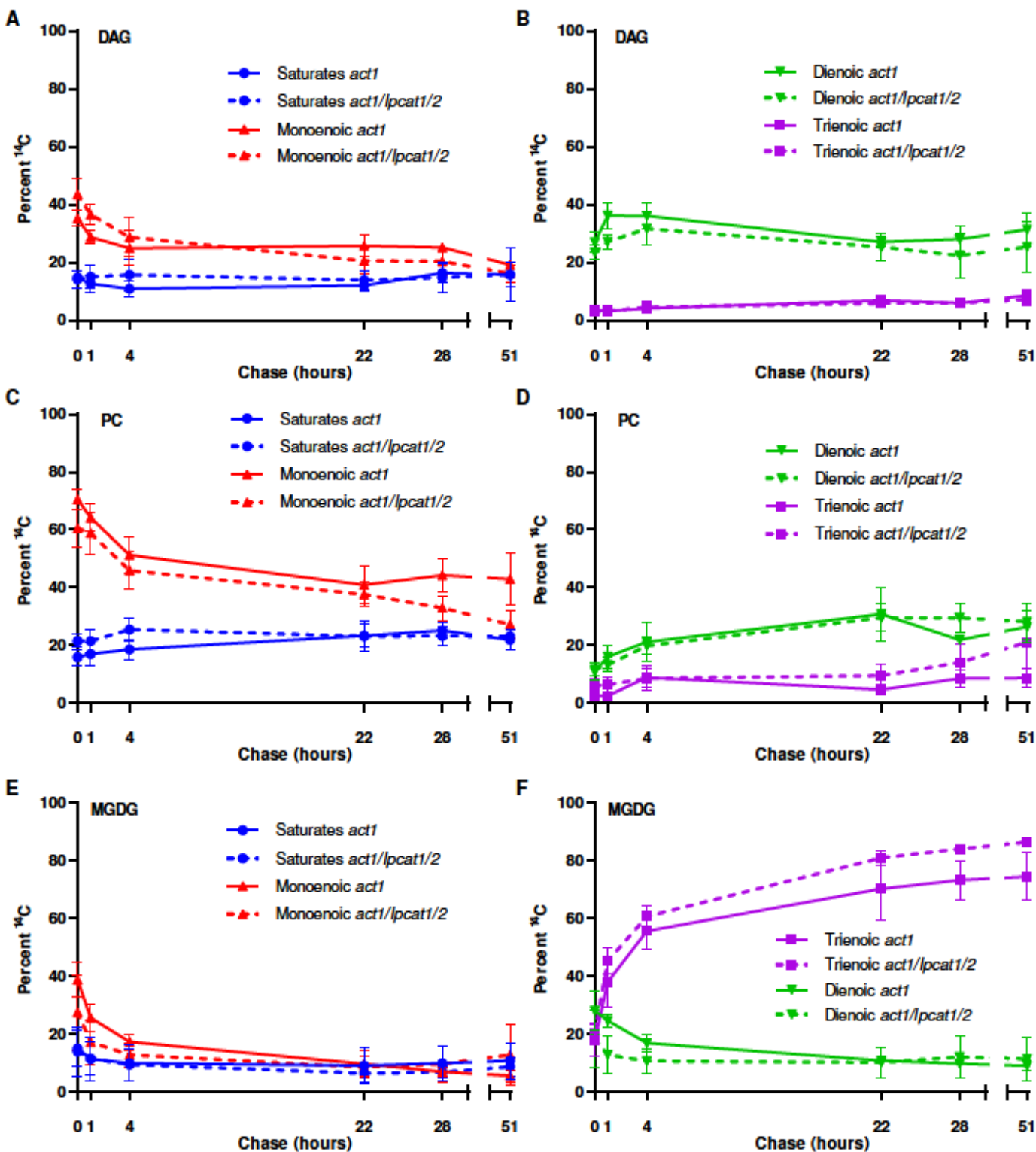
**Figure 6. Relative accumulation of [<sup>14</sup>C]acetate labeled nascent fatty acids into leaf lipids.** The relative labeling of individual lipids to the total labeled lipids in each line compared between lines. (A) PC. (B) DAG and PA. (C) PE, PG, and PI/PS. (D) MGDG. All data points are average and SEM from three sets of independently labeled plants. Significant differences (students t-test, p-value <0.05) in lipid labeling between lines at each time point is indicated by an asterisk above the data point. An  $\alpha$  above the data indicates a p-value <0.07.



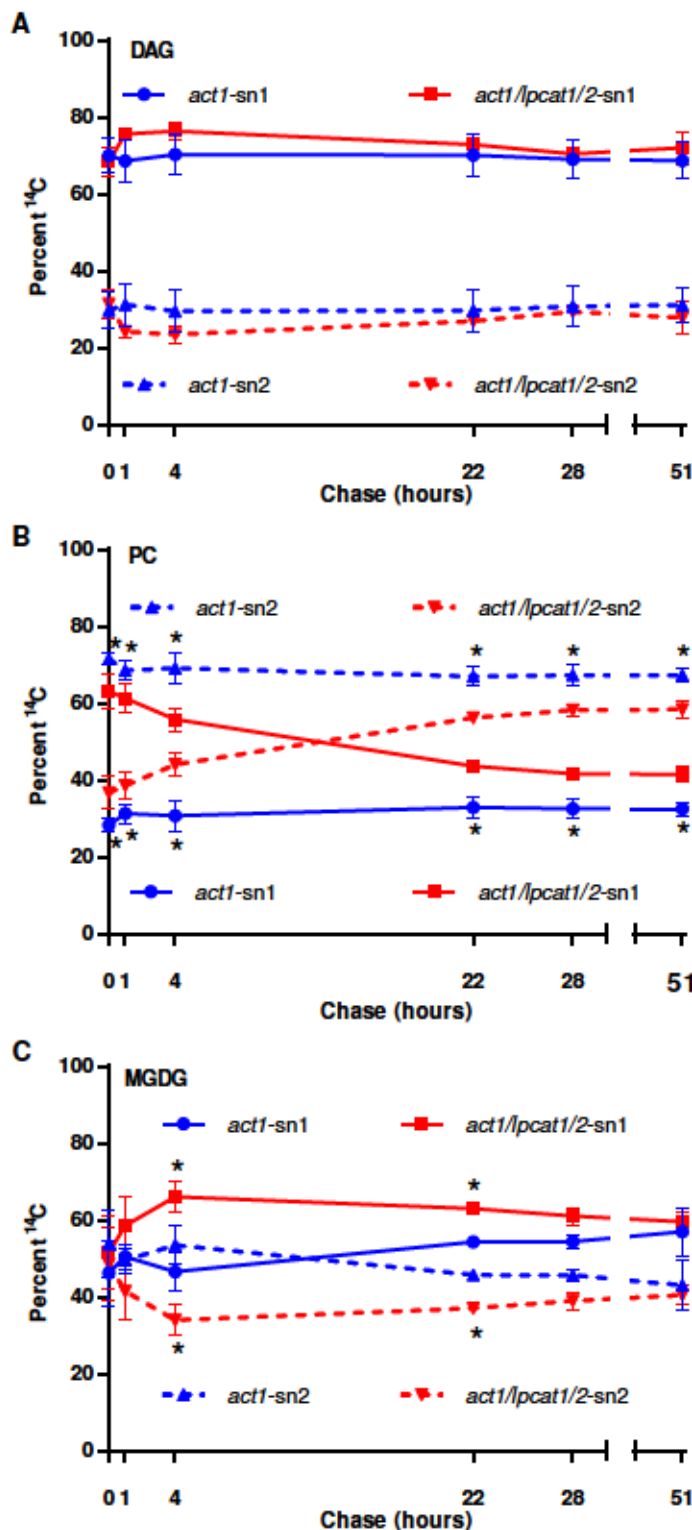
**Figure 7. Stereochemical analysis of [<sup>14</sup>C]acetate labeled nascent fatty acids incorporation into DAG and PC.** Continuous [<sup>14</sup>C]acetate labeled DAG and PC from Figures 5 and 6 were collected and subjected to lipase based regiochemical analysis of <sup>14</sup>C fatty acid locations in the sn-1 or sn-2 position of the glycerol backbone. (A) *act1* DAG. (B) *act1/lpcat1/2* DAG. (C) *act1* PC. (D) *act1/lpcat1/2* PC. All data points are average and SEM from three sets of independently labeled plants.



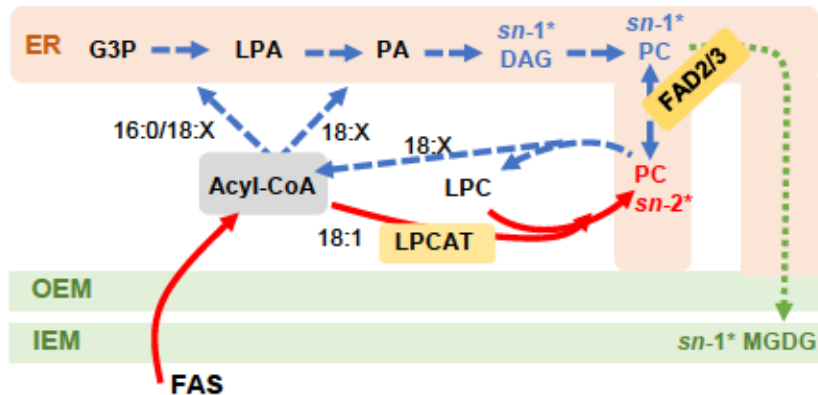
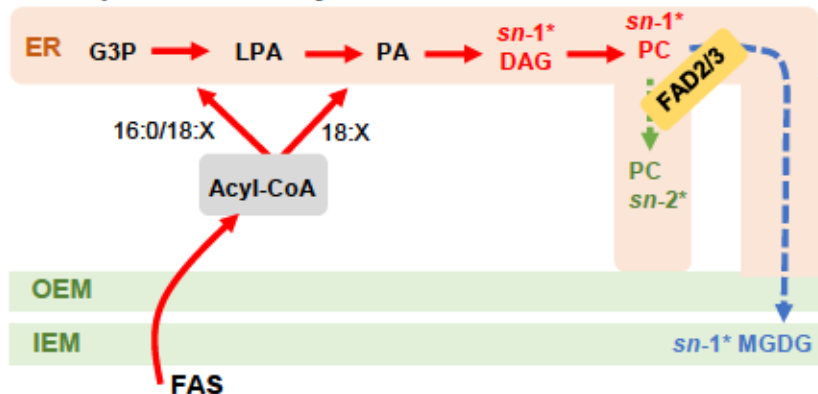
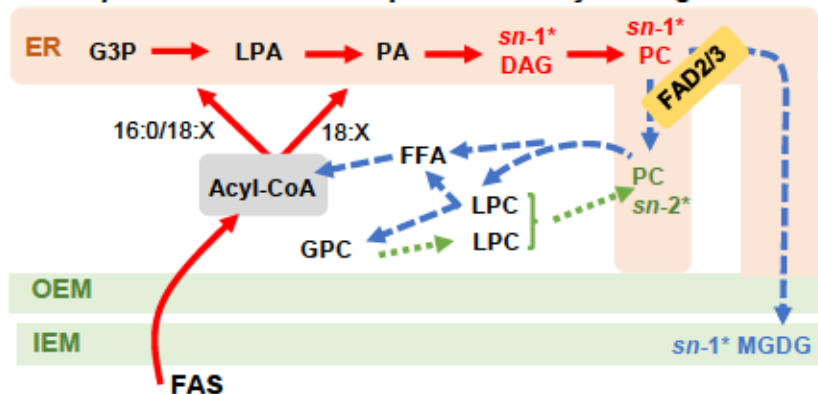
**Figure 8. Pulse-chase  $[^{14}\text{C}]$ acetate tracking of leaf lipid precursor-product relationships.** A 15 min  $[^{14}\text{C}]$ acetate pulse of 3 week old whole rosettes was followed by a chase up to 51 hours. (A-B) relative labeling of lipids within *act1* (A), or *act1/lpcat1/2* (B). (C-F), the relative labeling of major labeled individual lipids to the total labeled lipids in each line compared between lines. (C) PC and DAG. (D) MGDG. (E) PE and PA. (F) TAG. All data points are average and SEM from three sets of independently labeled plants, accept PA which is 1-3 reps. In (C-F), significant differences (students t-test,  $p$ -value  $<0.05$ ) in lipid labeling between lines at each time point is indicated by an asterisk above the data point.



**Figure 9. Radiolabeled fatty acid composition of DAG, PC, and MGDG over the [<sup>14</sup>C]acetate pulse-chase time course.** The radiolabeled fatty acids in different lipids from Fig. 8 are represented as total saturated fatty acids (e.g. 16:0, 18:0), monoenoic fatty acids (e.g. 18:1), dienoic (e.g. 18:2), and trienoic (e.g. 18:3). The proportion of each fatty acid within each lipid is compared between plant lines with *act1* as solid lines, and *act1/lpcat1/2* as dashed lines. (A-B) DAG. (C-D) PC. (E-F) MGDG. All data points are average and SEM from three sets of independently labeled plants from Fig. 8. Significant differences (students t-test, p-value <0.05) in lipid labeling between lines at each time point is indicated by an asterisk above the data point.



**Figure 10. Stereochemical analysis of [<sup>14</sup>C]acetate labeled fatty acids within DAG, PC, and MGDG over the pulse-chase time course.** The *sn*-1 position is solid lines, the *sn*-2 position is dashed lines. The *act1* samples are blue lines, the *act1/lpcat1/2* samples are red lines. (A) DAG. (B) PC. (C) MGDG. All data points are average and SEM from three sets of independently labeled plants from Fig. 8. Significant differences (students t-test, p-value <0.05) in lipid labeling between *act1* and *act1/lpcat1/2* stereochemical positions at each time point is indicated by an asterisk next to the *act1* blue lines in (B), and next to the *act1/lpcat1/2* red lines in (C).

**A: *act1*****B: *act1/lpcat1/2* no PC acyl removal****C: *act1/lpcat1/2* LPCAT1/2 independent PC acyl editing****Figure 11: Models of [<sup>14</sup>C]acetate pulse-chase labeling of MGDG synthesis in *act1* and *act1/lpcat1/2* leaves.**

The models indicate the relative rate of labeled fatty acid flux through the eukaryotic pathway of MGDG synthesis within the pulse-chase experiment. Red solid lines represent initial reactions, blue large dashed lines represent the next set of reactions labeled, the green small dashed lines represent the slowest set of reactions labeled within each model. Likewise, for the DAG, PC and MGDG pools, the major labeled stereochemical position at various time points is indicated by the position noted with an asterisk and color coding the same as the lines. No specific time points are intended and each model color coding is independent from the others, representing only relative labeling within each model. Abbreviations are as in the text. A, *act1*. B, *act1/lpcat1/2* with no PC acyl chain removal from residual acyl editing mechanisms. C, *act1/lpcat1/2* with compensating acyl editing reactions which lead to acyl chain removal from PC and incorporation into the acyl-CoA pool, and the switching of PC labeled stereochemistry from *sn*-1 to *sn*-2.

## Eukaryotic pathway

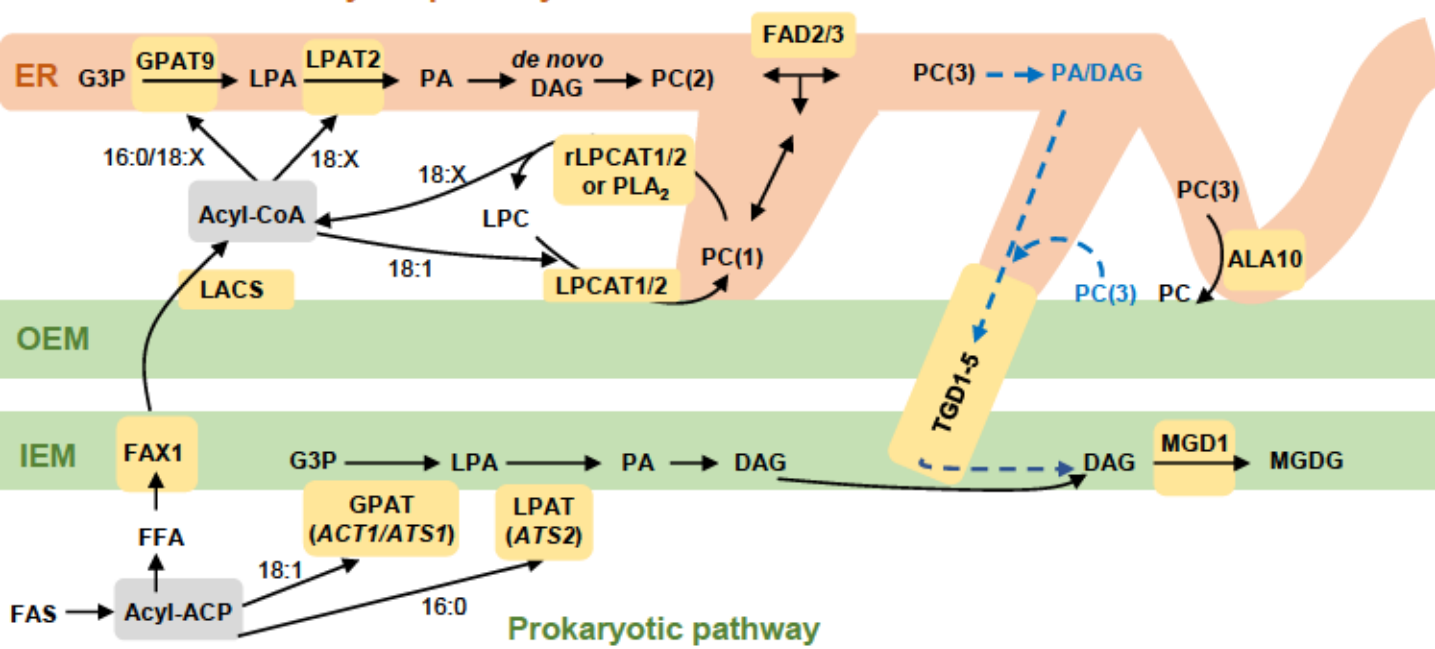


**Figure 12. Updated model of wild-type *Arabidopsis* acyl trafficking within leaf glycerolipid assembly clarifying the role of LPCAT1/2.**

The model focuses on the trafficking of acyl groups between the chloroplast and the ER for MGDG synthesis. Here the model separates PC involved in acyl editing “PC(1)” from PC synthesized *de novo* “PC(2)” and PC which provides the substrate for MGDG synthesis “PC(3)”. The model also allows that PC acyl editing may take place in the ER or at the chloroplast surface, which could be a way to move acyl groups into the ER by PC movement through membrane contact sites. The PC(3) pool is derived from *de novo* synthesized PC(2) which may have been further desaturated by FAD2/3. The substrate for MGDG synthesis may come from turnover of the PC(3) pool in the ER, or turnover of the PC(3) at the chloroplast surface. Key enzymes/transporters are in yellow, uncertain reactions are in blue and have dashed lines. Abbreviations are as in text, rLPCAT is the reverse LPCAT reaction.

## Parsed Citations

Allen, D.K., Bates, P.D., and Tjellström, H. (2015). Tracking the metabolic pulse of plant lipid production with isotopic labeling and flux analyses: Past, present and future. *Prog. Lipid Res.* 58, 97-120.  
PubMed: [Author and Title](#)  
Google Scholar: [Author Only Title Only Author and Title](#)

Andersson, M., and Dörmann, P. (2008). Chloroplast Membrane Lipid Biosynthesis and Transport. *The Chloroplast: Interactions with the Environment* 13, 125.  
PubMed: [Author and Title](#)  
Google Scholar: [Author Only Title Only Author and Title](#)

Andersson, M.X., Goksor, M., and Sandelius, A.S. (2007). Optical manipulation reveals strong attracting forces at membrane contact sites between endoplasmic reticulum and chloroplasts. *J Biol Chem* 282, 1170-1174.  
PubMed: [Author and Title](#)  
Google Scholar: [Author Only Title Only Author and Title](#)

Arnon, D.I. (1949). Copper enzymes in isolated chloroplasts - polyphenoloxidase in Beta-Vulgaris. *Plant Physiol.* 24, 1-15.  
PubMed: [Author and Title](#)  
Google Scholar: [Author Only Title Only Author and Title](#)

Arondel, V., Lemieux, B., Hwang, I., Gibson, S., Goodman, H.M., and Somerville, C.R. (1992). Map-based cloning of a gene controlling omega-3-fatty-acid desaturation in *Arabidopsis*. *Science* 258, 1353-1355.  
PubMed: [Author and Title](#)  
Google Scholar: [Author Only Title Only Author and Title](#)

Aulakh, K., and Durrett, T.P. (2019). The Plastid Lipase PLIP1 Is Critical for Seed Viability in *diacylglycerol acyltransferase1* Mutant Seed. *Plant Physiol.* 180, 1962-1974.  
PubMed: [Author and Title](#)  
Google Scholar: [Author Only Title Only Author and Title](#)

Awai, K., Xu, C.C., Tamot, B., and Benning, C. (2006). A phosphatidic acid-binding protein of the chloroplast inner envelope membrane involved in lipid trafficking. *Proc. Natl. Acad. Sci. U. S. A.* 103, 10817-10822.  
PubMed: [Author and Title](#)  
Google Scholar: [Author Only Title Only Author and Title](#)

Bastien, O., Botella, C., Chevalier, F., Block, M.A., Jouhet, J., Breton, C., Girard-Egrot, A., and Maréchal, E. (2016). Chapter One - New Insights on Thylakoid Biogenesis in Plant Cells. In *International Review of Cell and Molecular Biology*, K.W. Jeon, ed (Academic Press), pp. 1-30.  
PubMed: [Author and Title](#)  
Google Scholar: [Author Only Title Only Author and Title](#)

Bates, P.D. (2016). Understanding the control of acyl flux through the lipid metabolic network of plant oil biosynthesis. *Biochimica et Biophysica Acta (BBA) - Molecular and Cell Biology of Lipids* 1861, 1214-1225.  
PubMed: [Author and Title](#)  
Google Scholar: [Author Only Title Only Author and Title](#)

Bates, P.D., Ohlrogge, J.B., and Pollard, M. (2007). Incorporation of Newly Synthesized Fatty Acids into Cytosolic Glycerolipids in Pea Leaves Occurs via Acyl Editing. *J. Biol. Chem.* 282, 31206-31216.  
PubMed: [Author and Title](#)  
Google Scholar: [Author Only Title Only Author and Title](#)

Bates, P.D., Stymne, S., and Ohlrogge, J. (2013). Biochemical pathways in seed oil synthesis. *Curr. Opin. Plant Biol.* 16, 358-364.  
PubMed: [Author and Title](#)  
Google Scholar: [Author Only Title Only Author and Title](#)

Bates, P.D., Durrett, T.P., Ohlrogge, J.B., and Pollard, M. (2009). Analysis of Acyl Fluxes through Multiple Pathways of Triacylglycerol Synthesis in Developing Soybean Embryos. *Plant Physiol.* 150, 55-72.  
PubMed: [Author and Title](#)  
Google Scholar: [Author Only Title Only Author and Title](#)

Bates, P.D., Fatihi, A., Snapp, A.R., Carlsson, A.S., Browse, J., and Lu, C. (2012). Acyl editing and headgroup exchange are the major mechanisms that direct polyunsaturated fatty acid flux into triacylglycerols. *Plant Physiol.* 160, 1530-1539.  
PubMed: [Author and Title](#)  
Google Scholar: [Author Only Title Only Author and Title](#)

Benning, C. (2008). A role for lipid trafficking in chloroplast biogenesis. *Prog. Lipid Res.* 47, 381-389.  
PubMed: [Author and Title](#)  
Google Scholar: [Author Only Title Only Author and Title](#)

Benning, C. (2009). Mechanisms of Lipid Transport Involved in Organelle Biogenesis in Plant Cells. *Annu. Rev. Cell Dev. Biol.* 25, 71-91.  
PubMed: [Author and Title](#)  
Google Scholar: [Author Only Title Only Author and Title](#)

Bessoule, J.J., Testet, E., and Cassagne, C. (1995). Synthesis of phosphatidylcholine in the chloroplast envelope after import of lysophosphatidylcholine from endoplasmic reticulum membranes. *Eur. J. Biochem.* 228, 490-497.  
PubMed: [Author and Title](#)  
Google Scholar: [Author Only](#) [Title Only](#) [Author and Title](#)

Block, M.A., and Jouhet, J. (2015). Lipid trafficking at endoplasmic reticulum-chloroplast membrane contact sites. *Current Opinion in Cell Biology* 35, 21-29.  
PubMed: [Author and Title](#)  
Google Scholar: [Author Only](#) [Title Only](#) [Author and Title](#)

Botella, C., Jouhet, J., and Block, M.A. (2017). Importance of phosphatidylcholine on the chloroplast surface. *Prog Lipid Res* 65, 12-23.  
PubMed: [Author and Title](#)  
Google Scholar: [Author Only](#) [Title Only](#) [Author and Title](#)

Botella, C., Sautron, E., Boudière, L., Michaud, M., Dubots, E., Yamaryo-Botté, Y., Albrieux, C., Marechal, E., Block, M.A., and Jouhet, J. (2016). ALA10, a Phospholipid Flippase, Controls FAD2/FAD3 Desaturation of Phosphatidylcholine in the ER and Affects Chloroplast Lipid Composition in *Arabidopsis thaliana*. *Plant Physiol.* 170, 1300-1314.  
PubMed: [Author and Title](#)  
Google Scholar: [Author Only](#) [Title Only](#) [Author and Title](#)

Boudière, L., Michaud, M., Petroutsos, D., Rébeillé, F., Falconet, D., Bastien, O., Roy, S., Finazzi, G., Rolland, N., Jouhet, J., Block, M.A., and Maréchal, E. (2014). Glycerolipids in photosynthesis: Composition, synthesis and trafficking. *Biochimica et Biophysica Acta (BBA) - Bioenergetics* 1837, 470-480.  
PubMed: [Author and Title](#)  
Google Scholar: [Author Only](#) [Title Only](#) [Author and Title](#)

Browse, J., and Somerville, C. (1991). Glycerolipid synthesis - biochemistry and regulation. *Annu. Rev. Plant Physiol. Plant Molec. Biol.* 42, 467-506.  
PubMed: [Author and Title](#)  
Google Scholar: [Author Only](#) [Title Only](#) [Author and Title](#)

Browse, J., Warwick, N., Somerville, C.R., and Slack, C.R. (1986). Fluxes through the prokaryotic and eukaryotic pathways of lipid-synthesis in the 16:3 plant *Arabidopsis-thaliana*. *Biochem. J.* 235, 25-31.  
PubMed: [Author and Title](#)  
Google Scholar: [Author Only](#) [Title Only](#) [Author and Title](#)

Bulat, E., and Garrett, T.A. (2011). Putative N-Acylphosphatidylethanolamine Synthase from *Arabidopsis thaliana* Is a Lysoglycerophospholipid Acyltransferase. *J. Biol. Chem.* 286, 33819-33831.  
PubMed: [Author and Title](#)  
Google Scholar: [Author Only](#) [Title Only](#) [Author and Title](#)

Dorne, A.J., Joyard, J., Block, M.A., and Douce, R. (1985). Localization of phosphatidylcholine in outer envelope membrane of spinach chloroplasts. *The Journal of Cell Biology* 100, 1690-1697.  
PubMed: [Author and Title](#)  
Google Scholar: [Author Only](#) [Title Only](#) [Author and Title](#)

Fan, J., Yan, C., and Xu, C. (2013a). Phospholipid:diacylglycerol acyltransferase-mediated triacylglycerol biosynthesis is crucial for protection against fatty acid-induced cell death in growing tissues of *Arabidopsis*. *Plant J* 76, 930-942.  
PubMed: [Author and Title](#)  
Google Scholar: [Author Only](#) [Title Only](#) [Author and Title](#)

Fan, J., Yan, C., Zhang, X., and Xu, C. (2013b). Dual role for phospholipid:diacylglycerol acyltransferase: enhancing fatty acid synthesis and diverting fatty acids from membrane lipids to triacylglycerol in *Arabidopsis* leaves. *Plant Cell* 25, 3506-3518.  
PubMed: [Author and Title](#)  
Google Scholar: [Author Only](#) [Title Only](#) [Author and Title](#)

Fan, J., Zhai, Z., Yan, C., and Xu, C. (2015). *Arabidopsis* TRIGALACTOSYLDIACYLGLYCEROL5 interacts with TGD1, TGD2, and TGD4 to facilitate lipid transfer from the endoplasmic reticulum to plastids. *The Plant Cell*, tpc. 15.00394.  
PubMed: [Author and Title](#)  
Google Scholar: [Author Only](#) [Title Only](#) [Author and Title](#)

Fan, J., Yan, C., Roston, R., Shanklin, J., and Xu, C. (2014). *Arabidopsis* Lipins, PDAT1 Acyltransferase, and SDP1 Triacylglycerol Lipase Synergistically Direct Fatty Acids toward beta-Oxidation, Thereby Maintaining Membrane Lipid Homeostasis. *Plant Cell* 26, 4119-4134.  
PubMed: [Author and Title](#)  
Google Scholar: [Author Only](#) [Title Only](#) [Author and Title](#)

Głąb, B., Beganovic, M., Anaokar, S., Hao, M.-S., Rasmussen, A., Patton-Vogt, J., Banaś, A., Stymne, S., and Lager, I. (2016). Cloning of glycerophosphocholine acyltransferase (GPCAT) from fungi and plants; a novel enzyme in phosphatidylcholine synthesis. *J. Biol. Chem.* 291, 25066-25076.  
PubMed: [Author and Title](#)  
Google Scholar: [Author Only](#) [Title Only](#) [Author and Title](#)

Hara, A., and Radin, N.S. (1978). Lipid extraction of tissues with a low-toxicity solvent. *Anal. Biochem.* 90, 420-426.  
PubMed: [Author and Title](#)

Google Scholar: [Author Only](#) [Title Only](#) [Author and Title](#)

Hurlock, A.K., Roston, R.L., Wang, K., and Benning, C. (2014). Lipid Trafficking in Plant Cells. *Traffic* 15, 915-932.

Pubmed: [Author and Title](#)

Google Scholar: [Author Only](#) [Title Only](#) [Author and Title](#)

Hurlock, A.K., Wang, K., Takeuchi, T., Horn, P.J., and Benning, C. (2018). In vivo lipid 'tag and track' approach shows acyl editing of plastid lipids and chloroplast import of phosphatidylglycerol precursors in *Arabidopsis thaliana*. *Plant J* 95, 1129-1139.

Pubmed: [Author and Title](#)

Google Scholar: [Author Only](#) [Title Only](#) [Author and Title](#)

Jarvis, P., Dörmann, P., Peto, C.A., Lutes, J., Benning, C., and Chory, J. (2000). Galactolipid deficiency and abnormal chloroplast development in the *Arabidopsis MGD synthase 1* mutant. *Proceedings of the National Academy of Sciences* 97, 8175-8179.

Pubmed: [Author and Title](#)

Google Scholar: [Author Only](#) [Title Only](#) [Author and Title](#)

Jasieniecka-Gazarkiewicz, K., Demski, K., Lager, I., Stymne, S., and Banas, A. (2016). Possible Role of Different Yeast and Plant Lysophospholipid:Acyl-CoA Acyltransferases (LPLATs) in Acyl Remodelling of Phospholipids. *Lipids* 51, 15-23.

Pubmed: [Author and Title](#)

Google Scholar: [Author Only](#) [Title Only](#) [Author and Title](#)

Jessen, D., Roth, C., Wiermer, M., and Fulda, M. (2015). Two Activities of Long-Chain Acyl-Coenzyme A Synthetase Are Involved in Lipid Trafficking between the Endoplasmic Reticulum and the Plastid in *Arabidopsis*. *Plant Physiol.* 167, 351-366.

Pubmed: [Author and Title](#)

Google Scholar: [Author Only](#) [Title Only](#) [Author and Title](#)

Kelly, A.A., and Dörmann, P. (2004). Green light for galactolipid trafficking. *Curr Opin Plant Biol* 7, 262-269.

Pubmed: [Author and Title](#)

Google Scholar: [Author Only](#) [Title Only](#) [Author and Title](#)

Kim, H.U., Li, Y.B., and Huang, A.H.C. (2005). Ubiquitous and endoplasmic reticulum-located lysophosphatidyl acyltransferase, LPAT2, is essential for female but not male gametophyte development in *Arabidopsis*. *Plant Cell* 17, 1073-1089.

Pubmed: [Author and Title](#)

Google Scholar: [Author Only](#) [Title Only](#) [Author and Title](#)

Koo, A.J.K., Ohlrogge, J.B., and Pollard, M. (2004). On the export of fatty acids from the chloroplast. *J. Biol. Chem.* 279, 16101-16110.

Pubmed: [Author and Title](#)

Google Scholar: [Author Only](#) [Title Only](#) [Author and Title](#)

Kubis, S.E., Lilley, K.S., and Jarvis, P. (2008). Isolation and Preparation of Chloroplasts from *Arabidopsis thaliana* Plants. In 2D PAGE: Sample Preparation and Fractionation, A. Posch, ed (Totowa, NJ: Humana Press), pp. 171-186.

Pubmed: [Author and Title](#)

Google Scholar: [Author Only](#) [Title Only](#) [Author and Title](#)

Kunst, L., Browse, J., and Somerville, C. (1988). Altered regulation of lipid biosynthesis in a mutant of *Arabidopsis* deficient in chloroplast glycerol-3-phosphate acyltransferase activity. *Proc. Natl. Acad. Sci. U. S. A.* 85, 4143-4147.

Pubmed: [Author and Title](#)

Google Scholar: [Author Only](#) [Title Only](#) [Author and Title](#)

LaBrant, E., Barnes, A.C., and Roston, R.L. (2018). Lipid transport required to make lipids of photosynthetic membranes. *Photosynthesis Research*.

Pubmed: [Author and Title](#)

Google Scholar: [Author Only](#) [Title Only](#) [Author and Title](#)

Lager, I., Glab, B., Eriksson, L., Chen, G., Banas, A., and Stymne, S. (2015). Novel reactions in acyl editing of phosphatidylcholine by lysophosphatidylcholine transacylase (LPCT) and acyl-CoA:glycerophosphocholine acyltransferase (GPCAT) activities in microsomal preparations of plant tissues. *Planta* 241, 347-358.

Pubmed: [Author and Title](#)

Google Scholar: [Author Only](#) [Title Only](#) [Author and Title](#)

Lager, I., Yilmaz, J.L., Zhou, X.-R., Jasieniecka, K., Kazachkov, M., Wang, P., Zou, J., Weselake, R., Smith, M.A., Bayon, S., Dyer, J.M., Shockley, J.M., Heinz, E., Green, A., Banas, A., and Stymne, S. (2013). Plant Acyl-CoA:Lysophosphatidylcholine Acyltransferases (LPCATs) Have Different Specificities in Their Forward and Reverse Reactions. *J. Biol. Chem.* 288, 36902-36914.

Pubmed: [Author and Title](#)

Google Scholar: [Author Only](#) [Title Only](#) [Author and Title](#)

Lands, W.E.M. (1965). Lipid metabolism. *Annu. Rev. Biochem.* 34, 313-8.

Pubmed: [Author and Title](#)

Google Scholar: [Author Only](#) [Title Only](#) [Author and Title](#)

Larsson, K.E., Kjellberg, J.M., Tjellstrom, H., and Sandelius, A.S. (2007). LysoPC acyltransferase/PC transacylase activities in plant plasma membrane and plasma membrane-associated endoplasmic reticulum. *BMC Plant Biol.* 7, 12.

Pubmed: [Author and Title](#)

Google Scholar: [Author Only](#) [Title Only](#) [Author and Title](#)

Li-Beisson, Y., Neunzig, J., Lee, Y., and Philipp, K. (2017). Plant membrane-protein mediated intracellular traffic of fatty acids and acyl lipids. *Curr. Opin. Plant Biol.* 40, 138-146.

Pubmed: [Author and Title](#)

Google Scholar: [Author Only Title Only Author and Title](#)

Li-Beisson, Y., Shorrosh, B., Beisson, F., Andersson, M.X., Arondel, V., Bates, P.D., Baud, S., Bird, D., Debano, A., Durrett, T.P., Franke, R.B., Graham, I.A., Katayama, K., Kelly, A.A., Larson, T., Markham, J.E., Miquel, M., Molina, I., Nishida, I., Rowland, O., Samuels, L., Schmid, K.M., Wada, H., Welti, R., Xu, C., Zallot, R., and Ohlrogge, J. (2013). Acyl-lipid metabolism. *The Arabidopsis book / American Society of Plant Biologists* 11, e0161.

Pubmed: [Author and Title](#)

Google Scholar: [Author Only Title Only Author and Title](#)

Li, N., Gügel, I.L., Giavalisco, P., Zeisler, V., Schreiber, L., Soll, J., and Philipp, K. (2015). FAX1, a Novel Membrane Protein Mediating Plastid Fatty Acid Export. *PLoS Biol* 13, e1002053.

Pubmed: [Author and Title](#)

Google Scholar: [Author Only Title Only Author and Title](#)

Lu, B., and Benning, C. (2009). A 25-Amino Acid Sequence of the Arabidopsis TGD2 Protein Is Sufficient for Specific Binding of Phosphatidic Acid. *J. Biol. Chem.* 284, 17420-17427.

Pubmed: [Author and Title](#)

Google Scholar: [Author Only Title Only Author and Title](#)

Lu, B., Xu, C., Awai, K., Jones, A.D., and Benning, C. (2007). A small ATPase protein of Arabidopsis, TGD3, involved in chloroplast lipid import. *J. Biol. Chem.* 282, 35945-35953.

Pubmed: [Author and Title](#)

Google Scholar: [Author Only Title Only Author and Title](#)

Maatta, S., Scheu, B., Roth, M.R., Tamura, P., Li, M., Williams, T.D., Wang, X., and Welti, R. (2012). Levels of *Arabidopsis thaliana* leaf phosphatidic acids, phosphatidylserines, and most trienoate-containing polar lipid molecular species increase during the dark period of the diurnal cycle. *Frontiers in Plant Science* 3, 49.

Pubmed: [Author and Title](#)

Google Scholar: [Author Only Title Only Author and Title](#)

Maréchal, E., and Bastien, O. (2014). Modeling of regulatory loops controlling galactolipid biosynthesis in the inner envelope membrane of chloroplasts. *Journal of Theoretical Biology* 361, 1-13.

Pubmed: [Author and Title](#)

Google Scholar: [Author Only Title Only Author and Title](#)

Mei, C., Michaud, M., Cussac, M., Albrieux, C., Gros, V., Maréchal, E., Block, M.A., Jouhet, J., and Rébeillé, F. (2015). Levels of polyunsaturated fatty acids correlate with growth rate in plant cell cultures. *Scientific reports* 5, 15207.

Pubmed: [Author and Title](#)

Google Scholar: [Author Only Title Only Author and Title](#)

Mongrand, S., Bessoule, J.J., and Cassagne, C. (1997). A re-examination *in vivo* of the phosphatidylcholine-galactolipid metabolic relationship during plant lipid biosynthesis. *Biochem J.* 327, 853-858.

Pubmed: [Author and Title](#)

Google Scholar: [Author Only Title Only Author and Title](#)

Mongrand, S., Cassagne, C., and Bessoule, J.J. (2000). Import of lyso-phosphatidylcholine into chloroplasts likely at the origin of eukaryotic plastidial lipids. *Plant Physiol.* 122, 845-852.

Pubmed: [Author and Title](#)

Google Scholar: [Author Only Title Only Author and Title](#)

Mongrand, S., Bessoule, J.J., Cabantous, F., and Cassagne, C. (1998). The C-16 : 3/C-18 : 3 fatty acid balance in photosynthetic tissues from 468 plant species. *Phytochemistry* 49, 1049-1064.

Pubmed: [Author and Title](#)

Google Scholar: [Author Only Title Only Author and Title](#)

Moreau, P., Bessoule, J.J., Mongrand, S., Testet, E., Vincent, P., and Cassagne, C. (1998). Lipid trafficking in plant cells. *Prog. Lipid Res.* 37, 371-391.

Pubmed: [Author and Title](#)

Google Scholar: [Author Only Title Only Author and Title](#)

Mueller-Schuessele, S.J., and Michaud, M. (2018). Plastid Transient and Stable Interactions with Other Cell Compartments. In *Plastids: Methods and Protocols*, E. Maréchal, ed (New York, NY: Springer US), pp. 87-109.

Pubmed: [Author and Title](#)

Google Scholar: [Author Only Title Only Author and Title](#)

Nakamura, Y., Koizumi, R., Shui, G., Shimojima, M., Wenk, M.R., Ito, T., and Ohta, H. (2009). Arabidopsis lipins mediate eukaryotic pathway of lipid metabolism and cope critically with phosphate starvation. *Proceedings of the National Academy of Sciences*, -.

Pubmed: [Author and Title](#)

Google Scholar: [Author Only Title Only Author and Title](#)

Nishida, I., Tasaka, Y., Shiraishi, H., and Murata, N. (1993). The gene and the RNA for the precursor to the plastid-located glycerol-3-

phosphate acyltransferase of *Arabidopsis thaliana*. *Plant Mol Biol* 21, 267-277.

Pubmed: [Author and Title](#)

Google Scholar: [Author Only Title Only Author and Title](#)

Ohlrogge, J., and Browse, J. (1995). Lipid Biosynthesis. *Plant Cell* 7, 957-970.

Pubmed: [Author and Title](#)

Google Scholar: [Author Only Title Only Author and Title](#)

Okuley, J., Lightner, J., Feldmann, K., Yadav, N., Lark, E., and Browse, J. (1994). *Arabidopsis FAD2* gene encodes the enzyme that is essential for polyunsaturated lipid-synthesis. *Plant Cell* 6, 147-158.

Pubmed: [Author and Title](#)

Google Scholar: [Author Only Title Only Author and Title](#)

Roughan, P.G., and Slack, C.R. (1982). Cellular-organization of glycerolipid metabolism. *Annu. Rev. Plant Physiol. Plant Molec. Biol.* 33, 97-132.

Pubmed: [Author and Title](#)

Google Scholar: [Author Only Title Only Author and Title](#)

Schnurr, J.A., Shockley, J.M., de Boer, G.J., and Browse, J.A. (2002). Fatty acid export from the chloroplast. Molecular characterization of a major plastidial acyl-coenzyme A synthetase from *Arabidopsis*. *Plant Physiol* 129, 1700-1709.

Pubmed: [Author and Title](#)

Google Scholar: [Author Only Title Only Author and Title](#)

Shimojima, M., Ohta, H., and Nakamura, Y. (2009). Biosynthesis and function of chloroplast lipids. In *Lipids in Photosynthesis* (Springer), pp. 35-55.

Pubmed: [Author and Title](#)

Google Scholar: [Author Only Title Only Author and Title](#)

Shockley, J., Regmi, A., Cotton, K., Adhikari, N., Browse, J., and Bates, P.D. (2016). Identification of *Arabidopsis* GPAT9 (At5g60620) as an Essential Gene Involved in Triacylglycerol Biosynthesis. *Plant Physiol.* 170, 163-179.

Pubmed: [Author and Title](#)

Google Scholar: [Author Only Title Only Author and Title](#)

Singer, S.D., Chen, G., Mietkiewska, E., Tomasi, P., Jayawardhane, K., Dyer, J.M., and Weselake, R.J. (2016). *Arabidopsis* GPAT9 contributes to synthesis of intracellular glycerolipids but not surface lipids. *J Exp Bot* 67, 4627-4638.

Pubmed: [Author and Title](#)

Google Scholar: [Author Only Title Only Author and Title](#)

Slack, C.R., Roughan, P.G., and Balasingham, N. (1977). Labeling studies in vivo on metabolism of acyl and glycerol moieties of glycerolipids in developing maize leaf. *Biochem. J.* 162, 289-296.

Pubmed: [Author and Title](#)

Google Scholar: [Author Only Title Only Author and Title](#)

Stahl, U., Stalberg, K., Stymne, S., and Ronne, H. (2008). A family of eukaryotic lysophospholipid acyltransferases with broad specificity. *FEBS Lett* 582, 305-309.

Pubmed: [Author and Title](#)

Google Scholar: [Author Only Title Only Author and Title](#)

Stalberg, K., Stahl, U., Stymne, S., and Ohlrogge, J. (2009). Characterization of two *Arabidopsis thaliana* acyltransferases with preference for lysophosphatidylethanolamine. *BMC Plant Biol.* 9.

Pubmed: [Author and Title](#)

Google Scholar: [Author Only Title Only Author and Title](#)

Tjellström, H., Strawson, M., and Ohlrogge, J.B. (2015). Tracking synthesis and turnover of triacylglycerol in leaves. *J. Exp. Bot.* 66, 1453-1461.

Pubmed: [Author and Title](#)

Google Scholar: [Author Only Title Only Author and Title](#)

Tjellström, H., Yang, Z., Allen, D.K., and Ohlrogge, J.B. (2012). Rapid Kinetic Labeling of *Arabidopsis* Cell Suspension Cultures: Implications for Models of Lipid Export from Plastids. *Plant Physiol.* 158, 601-611.

Pubmed: [Author and Title](#)

Google Scholar: [Author Only Title Only Author and Title](#)

Wang, K., Froehlich, J.E., Zienkiewicz, A., Hersh, H.L., and Benning, C. (2017). A Plastid Phosphatidylglycerol Lipase Contributes to the Export of Acyl Groups from Plastids for Seed Oil Biosynthesis. *The Plant Cell* 29, 1678-1696.

Pubmed: [Author and Title](#)

Google Scholar: [Author Only Title Only Author and Title](#)

Wang, L., Kazachkov, M., Shen, W., Bai, M., Wu, H., and Zou, J. (2014). Deciphering the roles of *Arabidopsis* LPCAT and PAH in phosphatidylcholine homeostasis and pathway coordination for chloroplast lipid synthesis. *Plant J* 80, 965-976.

Pubmed: [Author and Title](#)

Google Scholar: [Author Only Title Only Author and Title](#)

Wang, L., Shen, W., Kazachkov, M., Chen, G., Chen, Q., Carlsson, A.S., Stymne, S., Weselake, R.J., and Zou, J. (2012a). Metabolic Interactions between the Lands Cycle and the Kennedy Pathway of Glycerolipid Synthesis in *Arabidopsis* Developing Seeds. *The Plant*

Cell Online 24, 4652-4669.

Pubmed: [Author and Title](#)

Google Scholar: [Author Only Title Only Author and Title](#)

Wang, Z., Xu, C., and Benning, C. (2012b). TGD4 involved in endoplasmic reticulum-to-chloroplast lipid trafficking is a phosphatidic acid binding protein. *The Plant Journal* 70, 614-623.

Pubmed: [Author and Title](#)

Google Scholar: [Author Only Title Only Author and Title](#)

Wang, Z., Anderson, N.S., and Benning, C. (2013). The Phosphatidic Acid Binding Site of the *Arabidopsis* Trigalactosyldiacylglycerol 4 (TGD4) Protein Required for Lipid Import into Chloroplasts. *J. Biol. Chem.* 288, 4763-4771.

Pubmed: [Author and Title](#)

Google Scholar: [Author Only Title Only Author and Title](#)

Williams, J.P., Imperial, V., Khan, M.U., and Hodson, J.N. (2000). The role of phosphatidylcholine in fatty acid exchange and desaturation in *Brassica napus* L. leaves. *Biochem. J.* 349, 127-133.

Pubmed: [Author and Title](#)

Google Scholar: [Author Only Title Only Author and Title](#)

Xu, C., and Shanklin, J. (2016). Triacylglycerol Metabolism, Function, and Accumulation in Plant Vegetative Tissues. *Annu. Rev. Plant Biol.* 67, 179-206.

Pubmed: [Author and Title](#)

Google Scholar: [Author Only Title Only Author and Title](#)

Xu, C., Fan, J., Froehlich, J.E., Awai, K., and Benning, C. (2005). Mutation of the TGD1 Chloroplast Envelope Protein Affects Phosphatidate Metabolism in *Arabidopsis*. *Plant Cell* 17, 3094-3110.

Pubmed: [Author and Title](#)

Google Scholar: [Author Only Title Only Author and Title](#)

Xu, C., Yu, B., Cornish, A.J., Froehlich, J.E., and Benning, C. (2006). Phosphatidylglycerol biosynthesis in chloroplasts of *Arabidopsis* mutants deficient in acyl-ACP glycerol-3- phosphate acyltransferase. *The Plant Journal* 47, 296-309.

Pubmed: [Author and Title](#)

Google Scholar: [Author Only Title Only Author and Title](#)

Xu, C.C., Fan, J.L., Riekhof, W., Froehlich, J.E., and Benning, C. (2003). A permease-like protein involved in ER to thylakoid lipid transfer in *Arabidopsis*. *Embo J.* 22, 2370-2379.

Pubmed: [Author and Title](#)

Google Scholar: [Author Only Title Only Author and Title](#)

Xu, J., Carlsson, A., Francis, T., Zhang, M., Hoffmann, T., Giblin, M., and Taylor, D. (2012). Triacylglycerol synthesis by PDAT1 in the absence of DGAT1 activity is dependent on re-acylation of LPC by LPCAT2. *BMC Plant Biol.* 12, 4.

Pubmed: [Author and Title](#)

Google Scholar: [Author Only Title Only Author and Title](#)

Yang, W., Wang, G., Li, J., Bates, P.D., Wang, X., and Allen, D.K. (2017). Phospholipase Dzeta Enhances Diacylglycerol Flux into Triacylglycerol. *Plant Physiol.* 174, 110-123.

Pubmed: [Author and Title](#)

Google Scholar: [Author Only Title Only Author and Title](#)

Yin, C., Andersson, M.X., Zhang, H., and Aronsson, H. (2015). Phosphatidylcholine is transferred from chemically-defined liposomes to chloroplasts through proteins of the chloroplast outer envelope membrane. *FEBS Lett.* 589, 177-181.

Pubmed: [Author and Title](#)

Google Scholar: [Author Only Title Only Author and Title](#)

Yu, B., Wakao, S., Fan, J., and Benning, C. (2004). Loss of Plastidic Lysophosphatidic Acid Acyltransferase Causes Embryo-Lethality in *Arabidopsis*. *Plant Cell Physiol.* 45, 503-510.

Pubmed: [Author and Title](#)

Google Scholar: [Author Only Title Only Author and Title](#)

Zhao, L., Katavic, V., Li, F., Haughn, G.W., and Kunst, L. (2010). Insertional mutant analysis reveals that long-chain acyl-CoA synthetase 1 (LACS1), but not LACS8, functionally overlaps with LACS9 in *Arabidopsis* seed oil biosynthesis. *Plant J.* 64, 1048-1058.

Pubmed: [Author and Title](#)

Google Scholar: [Author Only Title Only Author and Title](#)